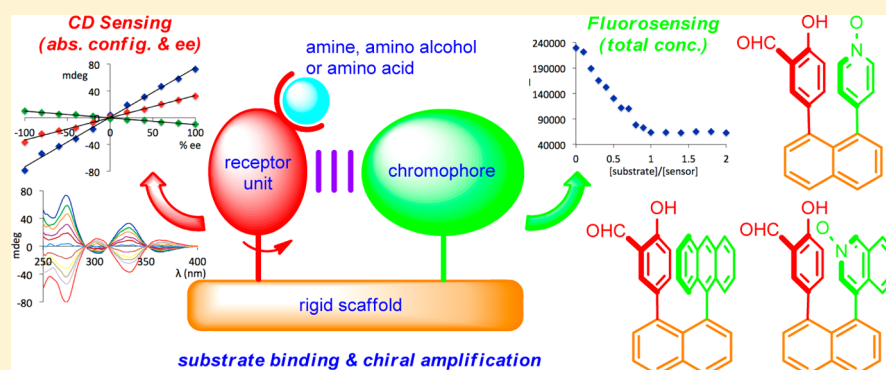# Comprehensive Chirality Sensing: Development of Stereodynamic Probes with a Dual (Chir)optical Response

Keith W. Bentley and Christian Wolf*

Department of Chemistry, Georgetown University, Washington, D.C. 20057, United States

Ⓢ *Supporting Information*

ABSTRACT: The attachment of a salicylaldehyde ring and a cofacial aryl or heteroaryl *N*-oxide chromophore onto a naphthalene scaffold affords stereodynamic probes designed to rapidly bind amines, amino alcohols, or amino acids and to translate this binding event via substrate-to-receptor chirality amplification into a dual (chir)optical response. 1-(3′-Formyl-4′-hydroxyphenyl)-8-(9′-anthryl)naphthalene (**1**) was prepared via two consecutive Suzuki cross-coupling reactions, and the three-dimensional structure and racemization kinetics were studied by crystallography and dynamic HPLC. This probe proved successful for chirality sensing of several compounds, but in situ IR monitoring of the condensation reaction between the salicylaldehyde moiety in **1** and phenylglycinol showed that the imine formation takes 2 h. Optimization of the substrate binding rate and the circular dichroism (CD) and fluorescence readouts led to the replacement of anthracene with smaller fluorophores capable of intramolecular hydrogen bonding. 1-(3′-Formyl-4′-methoxyphenyl)-8-(4′-isoquinolyl)naphthalene *N*-oxide (**2**) and its pyridyl analogue **3** combine fast substrate binding with distinctive chiral amplification. This asymmetric transformation of the first kind prompts CD and fluorescence responses that can be used for in situ determination of the absolute configuration, ee, and total concentration of many compounds. The general utility of the three chemosensors was successfully tested on 18 substrates.

■ INTRODUCTION

The amplification and sensing of molecular chirality play an increasingly important role in the advancement of asymmetric catalysis, biomedical treatments and diagnostics, material sciences, and other fields. The synthesis and stereochemical analysis of chiral compounds have developed into rapidly growing, mutually dependent fields that are of vital importance throughout the chemical sciences. The general availability of numerous chiral catalysts that can be tested in an enantioselective reaction together with the challenge to assess unpredictable effects of solvents, counterions, temperature, additives, and other reaction parameters on the chemical yield and stereoselectivity has directed increasing attention to high-throughput screening (HTS) efforts. As a result, progress in method development often relies on automated parallel synthesis that quickly generates hundreds of samples, while the analytical task, that is, the determination of the reaction yield and product ee, typically remains laborious and time-consuming. Chiroptical assays have been considered particularly promising to address this bottleneck.[1] Nakanishi and Berova showed more than 20 years ago that porphyrin receptors exhibiting induced circular dichroism (CD) can be used for the determination of the absolute configuration of chiral compounds.[2] Since then, a variety of stereodynamic chirality sensors have been introduced by Rosini,[3] Anslyn,[4] Canary,[4d,e,5] Borhan,[6] Toniolo,[7] Gawronski,[8] our group,[9] and others.[10]

The simultaneous determination of the absolute configuration, concentration, and enantiomeric composition of a chiral compound with an optical sensor is a challenging task. Our efforts to develop a probe that can accomplish such a complete stereochemical analysis have directed us to a dual sensing mode design that can provide an instant CD signal and either a UV or a fluorescence readout upon detection of a chiral substrate.[9i] As is shown in Scheme 1, a stereodynamic receptor moiety and a chromophore are connected in close proximity to a rigid scaffold to establish communication between the two units. The underlying idea is to couple a fast substrate recognition event

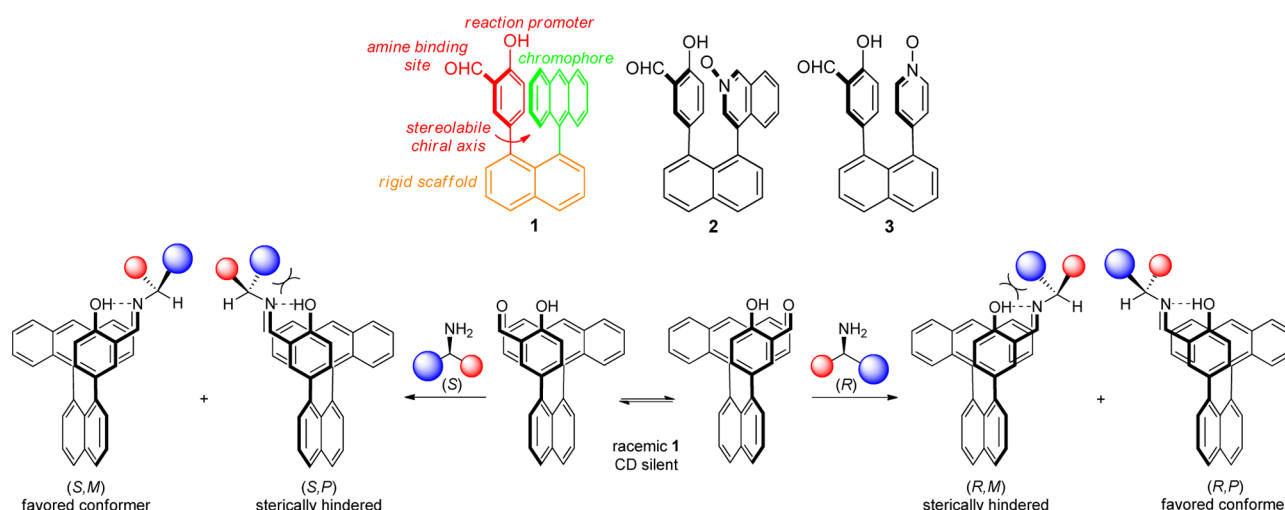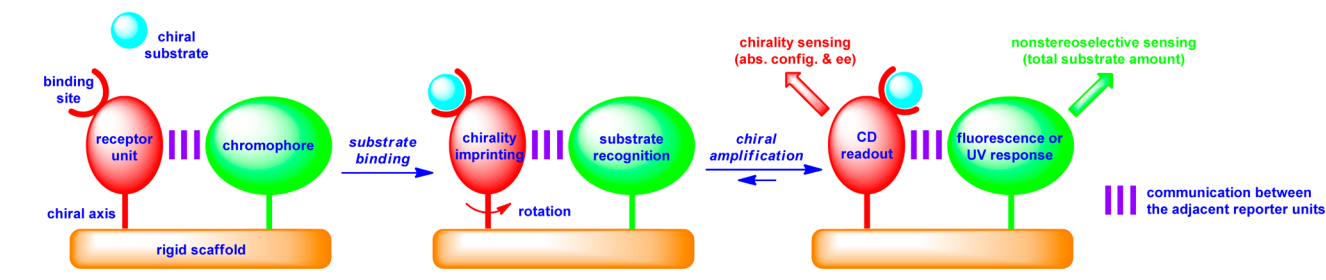**Scheme 1. Illustration of the Dual Sensing Mode Strategy**

Figure 1. Top: Structures of chemosensors **1**−**3** exhibiting a salicylaldehyde unit for ee determination and a proximate chromophore for total concentration analysis. Bottom: Imprinting of the chirality of amine substrates on the stereodynamic scaffold of sensor **1**.

Scheme 2. Synthesis of 1 and Crystal Structures of Intermediates 4 and 5[a]
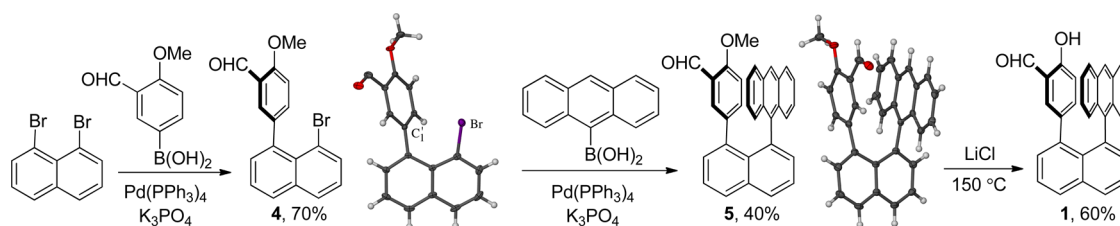
[a]Selected crystallographic measurements of **4**: C_1'−Br separation, 3.108 Å; twisting angle, 24.4°; splaying angle, 10.0°. Selected crystallographic measurements of **5**: phenyl$_{centroid}$−anthryl$_{centroid}$, 3.311 Å; twisting angle, 23.6°; splaying angle, 8.0°.

with a chiral amplification process at the receptor site. In the absence of a chiral bias, the probe exhibiting a stereolabile chiral axis exists as a mixture of rapidly interconverting stereoisomers and remains CD-silent. Binding of a chiral substrate at the stereodynamic receptor unit and subsequent chirality imprinting disturb this equilibrium and favor population of an axially chiral conformation. This could be measured by CD analysis and thus provide an entry to the determination of the absolute configuration and ee of the substrate. Communication of the binding event between the receptor part and the adjacent chromophore would concomitantly affect the UV or fluorescence properties of the chemosensor. This change would be independent of the substrate chirality and allow nonstereoselective sensing of the total substrate amount. To become practical for HTS purposes, the processes described above have to occur within a few minutes and generate strong (chir)optical responses that can be accurately quantified.

RESULTS AND DISCUSSION

We envisioned that a salicylaldehyde moiety connected via a stereolabile chiral axis to a naphthalene scaffold could function both as a receptor for a wide range of important chiral compounds carrying an amino group (amines, amino alcohols, and amino acids) and as the stereodynamic reporter unit (Figure 1). The acidic phenol function adjacent to the formyl group in the salicaldehyde ring was expected to accelerate the substrate binding process and allow for time-efficient chemosensing. The formation of a rigid imine product would then induce an asymmetric transformation of the first kind, generating a stereochemical bias at the chiral aryl−aryl axis in the sensor and a distinct CD signal. For example, the binding of an *R*-configured amine would favor population of the *R,P* conformer to avoid repulsion between the steric bulk of the bound substrate and the proximate chromophore. This central-to-axial chirality induction process thus disturbs the conformational equilibrium of the stereodynamic sensor and affords a quantifiable CD
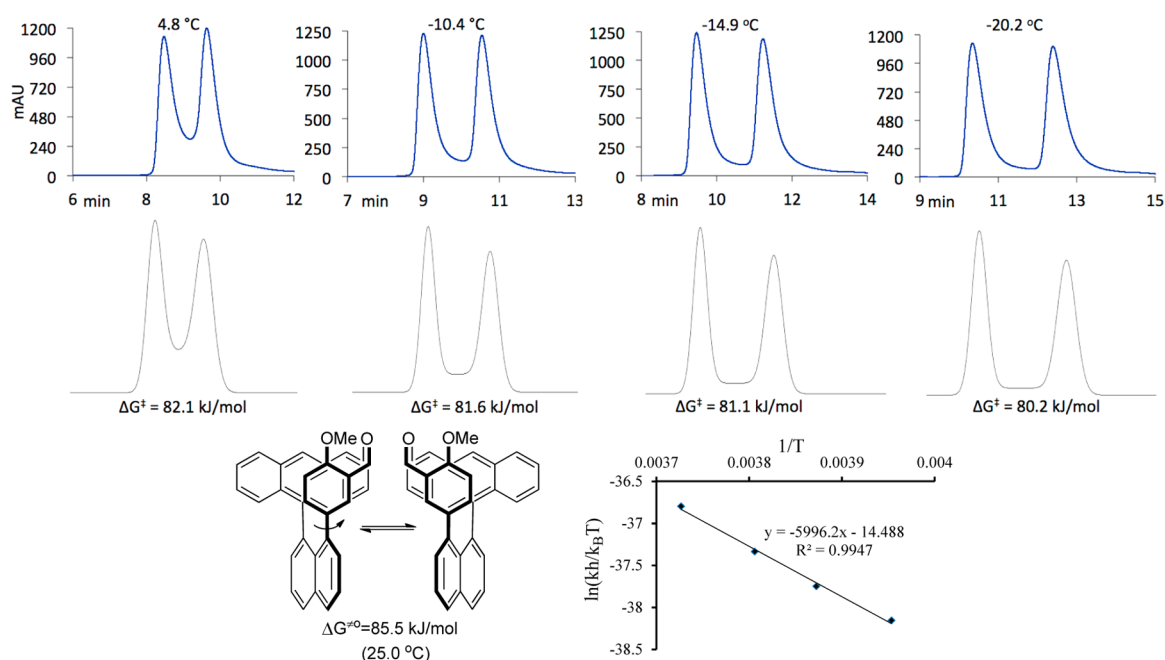
Figure 2. Top: Experimentally obtained HPLC chromatograms of compound **5** at four different temperatures. HPLC conditions: (*S*,*S*)-Whelk-O 1 (25 cm × 4.6 mm); mobile phase, CH_2Cl_2/hexanes (1:1); flow rate, 1 mL/min; UV detection, 254 nm. Bottom: Simulation of the elution profiles calculated with Mimesis 3.1 and the Eyring plot, which yielded $\Delta S^{\ddagger} = -120.5$ J mol^{-1} K^{-1}, $\Delta H^{\ddagger} = 49.9$ kJ/mol, and $\Delta G^{\ddagger\circ} = 85.8$ kJ/mol at 298.15 K.

response that is ultimately controlled by the bound substrate. The consideration of a large chromophoric group as the second reporter unit led to the structure of **1**. The placement of anthracene at the neighboring peri position in the naphthalene ring was expected to enforce a cofacial orientation and $\pi-\pi$ interactions between the two reporter units. As a result, the substrate recognition would be communicated from the salicylidenimine to the anthracene moiety via steric, dipole, and π-stacking interactions and thus alter the UV and fluorescence output of the sensor. This change would be independent of the chirality of the bound amino compound and afford a means to determine the total substrate amount. We now describe the development of dual mode sensors **1**−**3** and their use for the simultaneous determination of the absolute configuration, ee, and amount of a wide variety of unprotected chiral amines, amino alcohols, and amino acids.

Synthesis, Racemization Kinetics, and Chirality Sensing with Chemosensor 1. The synthesis of 1-(3′-formyl-4′-hydroxyphenyl)-8-(9′-anthryl)naphthalene (**1**) required careful optimization of two consecutive cross-coupling reactions (Scheme 2). Initial attempts to prepare 1-(3′-formyl-4′-methoxyphenyl)-8-bromonaphthalene (**4**) from 3-formyl-4-methoxyphenylboronic acid and 1,8-dibromonaphthalene by means of typical Suzuki coupling protocols gave low yields and large amounts of the debrominated and disubstituted derivatives. In an effort to improve the selectivity toward **4**, we carefully screened various palladium catalysts and optimized the solvent composition, base, temperature, and reaction time. We finally found that **4** can be obtained in 70% yield when the reaction is performed with 7.5 mol % Pd(PPh$_3$)$_4$ and 5 equiv of K$_3$PO$_4$ in a toluene/ethanol/water (3:2:1) mixture at 80 °C for 4 h. When the subsequent reaction of **4** and anthracene-9-boronic acid was carried out under the same conditions, only debromination was observed. However, several changes, including an increase in the catalyst loading, reaction time, and temperature, finally afforded the sterically crowded triaryl **5** carrying two cofacial aryl rings

perpendicular to the naphthalene scaffold.[11] To our surprise, several attempts to remove the methoxy group following a range of literature protocols with BBr$_3$,[9a] MgCl$_2$,[12] CeCl$_3$,[13] and AlCl$_3$[14] were unsuccessful. We were pleased to find that the use of LiCl in refluxing DMF produces **1** in 60% yield.[15]

The difficulties encountered during the synthesis of **4** and **5** are a result of the steric strain and repulsion between the two peri substituents. Crystallographic analysis of **4** reveals that the salicylaldehyde unit and the bromine are forced out of the naphthalene plane and spread apart from one another (Scheme 2). The twisting angle between the naphthalene−salicylaldehyde bond and the naphthalene−bromine bond was determined to be 24.4°. In addition, the two bonds are splayed by 10.0°. While the two aryl units in **5** are cofacial and perpendicular to the naphthalene plane as expected, the crystal structure shows twisting and a similar splaying as observed with **4**. The proximate anthracene ring also reduces the accessibility of the methoxy group on the adjacent salicylaldehyde ring and therefore severely hampers the demethylation reaction unless severe conditions are applied.

Having established synthetic access to the sterically crowded triaryl arrangement of **1** as well as crystallographic information about the three-dimensional structure, we continued with the determination of the activation free energy, $\Delta G^{\ddagger}$, for the rotation of the salicylaldehyde unit about the chiral aryl−aryl axis. We were unable to separate the rotational isomers of **1** by HPLC using a variety of chiral columns even at very low temperatures. However, the enantiomers of precursor **5** were resolved on the (*S*,*S*)-Whelk-O 1 chiral stationary phase using dichloromethane/hexanes (1:1) as the mobile phase (Figure 2). At −20 °C, the enantiomers have retention times of 10.3 and 12.4 min, and a small plateau between the peaks due to on-column racemization was observed. As expected, the height of the plateau increased as the temperature was raised stepwise to −5 °C. Simulation of the elution profiles at four different temperatures provided the corresponding enantiomerization rates obeying reversible first-
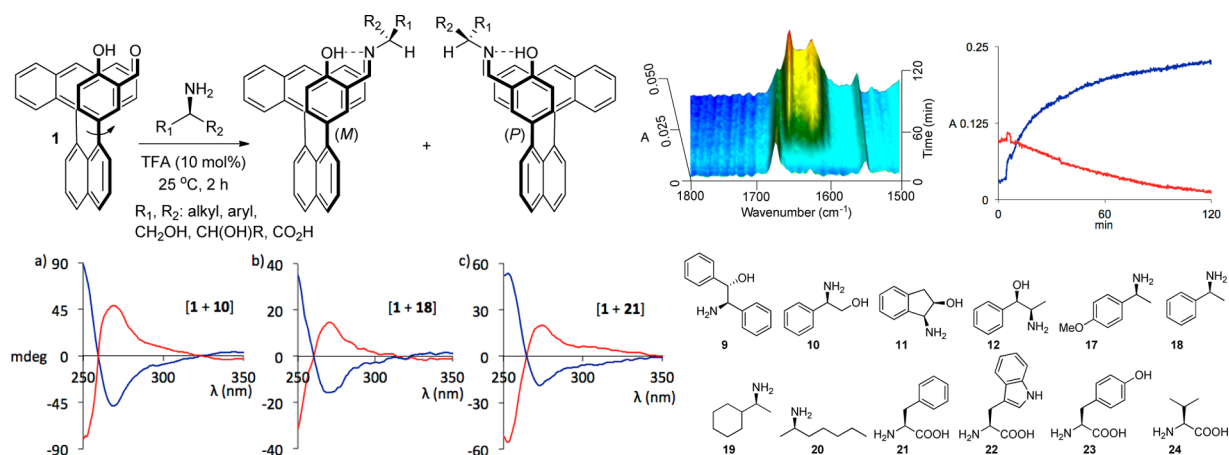
Figure 3. Top: Binding of amine substrates by sensor **1** and in situ IR analysis of the condensation reaction between **1** and **10**. The disappearance of **1** was measured by the decrease in the absorbance intensity of the aldehyde stretching at 1668 cm^{-1} (red), and the generation of the imine was monitored by the increase in the absorbance intensity of the imine stretching at 1635 cm^{-1} (blue). Bottom left: (a) CD spectra of the imines obtained from **1** and (*R*)-**10** (blue) and (*S*)-**10** (red). (b) CD spectra of the imines obtained from **1** and (*R*)-**18** (blue) and (*S*)-**18** (red). (c) CD spectra of the imines obtained from **1** and (*R*)-**21** (blue) and (*S*)-**21** (red). All of the spectra were collected at 7.5×10^{-5} M in MeOH (**10** and **18**) or CHCl$_3$ (**21**). Bottom right: Substrate scope of sensor **1**. Only one enantiomer is shown.

order kinetics. Eyring plot analysis gave an activation enthalpy, $\Delta H^{\ddagger}$, of 49.9 kJ/mol and an activation entropy, $\Delta S^{\ddagger}$, of −120.5 J mol^{-1} K^{-1}. The strikingly negative $\Delta S^{\ddagger}$ value corresponds well to a highly ordered T-shaped transition state in which the salicylaldehyde ring rotates through the naphthalene plane and is perpendicular to the adjacent anthracene moiety.[16] The standard activation free energy, $\Delta G^{\ddagger\circ}$, was calculated as 85.8 kJ/mol, which demonstrates that **5** and consequently the demethylated analogue **1** undergo rapid racemization at room temperature.
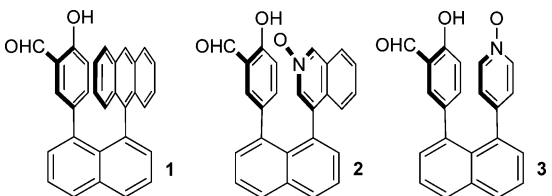
We envisioned that fixation of a chiral amine or amino alcohol by the salicylaldehyde unit would generate a rigid salicylidenimine motif stabilized by intramolecular hydrogen bonding. On the basis of the stereodynamic nature of **1**, that is, the rapid interconversion of the enantiomeric rotamers at room temperature, this would result in a spontaneous asymmetric transformation of the first kind favoring an axially chiral conformer that carries the bulkiest group of the bound substrate pointing away from the neighboring anthracene ring to occupy the least sterically hindered space. The imprinting of the substrate chirality on the conformational equilibrium of **1** was thus expected to generate a predominant sense of axial chirality and a characteristic CD response of the chemosensor. Despite the proximity of the acidic phenol moiety, the condensation reaction of **1** and phenylglycinol (**10**) at room temperature required 24 h to come to completion according to ^{1}H NMR analysis. However, the addition of 10 mol % trifluoroacetic acid to an equimolar mixture of **1** and **10** in chloroform significantly reduced the reaction time (Figure 3).[17] In-situ IR measurements showed that the formyl stretching of the sensor (1668 cm^{-1}) rapidly decreases and almost completely disappears within 2 h while the imine stretching of the condensation product (1635 cm^{-1}) reaches a maximum intensity. These results were confirmed by NMR and MS analysis (see the Supporting Information).

The CD spectra of the imines obtained from **1** and the enantiomers of **10** are shown in Figure 3. As expected, the stereodynamic chemosensor shows a strong chiroptical signal upon binding of the substrate, which is CD-silent in the absence of **1** under otherwise the same conditions. It is known that salicylidenimines can exist in the form of a quinoid-like structure

exhibiting CD signals at low wavelengths. In accordance with a previous study,[9a] we believe that the CD responses observed with sensor **1** originate from the relative orientation of the two cofacial chromophores, which are almost perfectly perpendicular to the naphthalene plane. A variety of amino alcohols were then tested to evaluate the general utility of **1** for enantioselective sensing. All of the condensation reactions were conducted in chloroform in the presence of catalytic amounts of trifluoroacetic acid and stirred for 5 h prior to CD analysis. The CD spectra were collected at micromolar concentrations, with alcoholic solvents such as methanol, ethanol, and isopropanol giving the strongest signals (see the Experimental Section). The imines derived from amino alcohols **9−12** generally exhibit strong CD signals above 250 nm, and the absolute configurations can be correlated to the CD spectra, with the *R* configuration generating a negative maximum at 270 nm and the *S* configuration generating a positive CD response at the same wavelength (Table 1 and the Supporting Information). Encouraged by the success with chemosensing of amino alcohols, we decided to pursue other classes of compounds bearing an amino function, namely, amines **17−20** and amino acids **21−24** (Figure 3). While the amine sensing was conducted as described above, the condensations with amino acids were performed in DMSO in the presence of 1 equiv of tetrabutylammonium hydroxide (TBAOH) to improve the solubility of the substrates. Again, characteristic Cotton effects were observed using the stereodynamic probe **1** for chirality sensing of a variety of aliphatic and aromatic amines and amino acids. A close comparison of the CD spectra reveals that all 12 substrates representing important amines, amino alcohols, and amino acids consistently generate a similar chiroptical response of **1**, namely, a strong positive CD signal at 270 nm when a substrate with the *S* configuration is used and the opposite (negative) Cotton effect when the corresponding *R* enantiomer is used (entries 1−12 in Table 1).

As mentioned above, the determination of the absolute configuration, ee, and total concentration of chiral compounds with a single chemosensor would afford a practical entry to a complete stereochemical analysis and be most valuable for high-throughput screening applications. Since the chiroptical studies conducted with chemosensor **1** established its general suitability

**Table 1. Summary of the CD Sensing Results with Chemosensors 1, 2, and 3**

entry	sensor	substrate class	substrate	Δ^a (mdeg)	predicted sign[b]
1	1	AA	(1S,2R)-9	−49	−
	1	AA	(1R,2S)-9	+55	+
2	1	AA	(R)-10	−48	−
	1	AA	(S)-10	+48	+
3	1	AA	(1R,2R)-11	−7	−
	1	AA	(1S,2S)-11	+7	+
4	1	AA	(1S,2R)-12	−9	−
	1	AA	(1R,2S)-12	+12	+
5	1	MA	(R)-17	−12	−
	1	MA	(S)-17	+11	+
6	1	MA	(R)-18	−15	−
	1	MA	(S)-18	+15	+
7	1	MA	(R)-19	−9	−
	1	MA	(S)-19	+10	+
8	1	MA	(R)-20	−5	−
	1	MA	(S)-20	+6	+
9	1	AC	(R)-21	−19	−
	1	AC	(S)-21	+20	+
10	1	AC	(R)-22	−10	−
	1	AC	(S)-22	+11	+
11	1	AC	(R)-23	−24	−
	1	AC	(S)-23	+24	+
12	1	AC	(R)-24	−10	−
	1	AC	(S)-24	+12	+
13	2	AA	(1S,2R)-9	+13	+
	2	AA	(1R,2S)-9	−13	−
14	2	AA	(R)-10	+13	+
	2	AA	(S)-10	−9	−
15	2	AA	(1R,2R)-11	+8	+
	2	AA	(1S,2S)-11	−8	−
16	2	AA	(1S,2R)-12	+3	+
	2	AA	(1R,2S)-12	−3	−
17	2	AA	(R)-13	+19	+
	2	AA	(S)-13	−19	−
18	2	AA	(R)-14	+12	+
	2	AA	(S)-14	−14	−
19	2	AA	(R)-15	+13	+
	2	AA	(S)-15	−13	−

entry	sensor	substrate class	substrate	Δ^a (mdeg)	predicted sign[b]
20	2	AA	(R)-16	+16	+
	2	AA	(S)-16	−15	−
21	2	AC	(R)-21	+19	+
	2	AC	(S)-21	−15	−
22	2	AC	(R)-22	+21	+
	2	AC	(S)-22	−27	−
23	2	AC	(R)-23	+19	+
	2	AC	(S)-23	−16	−
24	2	AC	(R)-24	+8	+
	2	AC	(S)-24	−11	−
25	3[c]	AA	(1S,2R)-9	+29	+
	3[c]	AA	(1R,2S)-9	−33	−
26	3[c]	AA	(R)-10	+77	+
	3[c]	AA	(S)-10	−78	−
27	3[c]	AA	(1R,2R)-11	+27	+
	3[c]	AA	(1S,2S)-11	−27	−
28	3[c]	AA	(1S,2R)-12	+61	+
	3[c]	AA	(1R,2S)-12	−63	−
29	3[c]	AA	(R)-13	+18	+
	3[c]	AA	(S)-13	−17	−
30	3[c]	AA	(R)-14	+57	+
	3[c]	AA	(S)-14	−47	−
31	3[c]	AA	(R)-15	+55	+
	3[c]	AA	(S)-15	−53	−
32	3[c]	AA	(R)-16	+63	+
	3[c]	AA	(S)-16	−66	−
33	3[c]	AA	(1R,2R)-28	+20	+
	3[c]	AA	(1S,2S)-28	−21	−
34	3	AC	(R)-21	+22	+
	3	AC	(S)-21	−22	−
35	3	AC	(R)-22	+36	+
	3	AC	(S)-22	−42	−
36	3	AC	(R)-23	+51	+
	3	AC	(S)-23	−42	−
37	3	AC	(R)-29	+22	+
	3	AC	(S)-29	−22	−

[a]CD output at 270 nm for sensor **1** and 260 nm for sensors **2** and **3**. The CD response to **28** was measured at 280 nm. [b]Predicted CD sign at 270 nm for sensor **1**, where R is negative and S is positive. Analysis of the CD readout at 260 nm for sensors **2** and **3** shows that R enantiomers give a positive sign and S substrates give a negative CD response for all substrates. MA = monoamine, AA = amino alcohol, AC = amino acid. [c]Reference 9i.

for enantioselective detection and possibly quantitative ee analysis of amino alcohols, amines, and amino acids, we decided to explore whether a change in the UV or fluorescence signal of **1** upon substrate binding would provide a means to determine the substrate concentration independent of the enantiomeric composition. Because the conversion of the salicylaldehyde to a salicylidenimine moiety ultimately alters its steric bulk, dipole moment, and π-stacking interactions, we expected that the substrate binding event would affect not only the conformational bias of the chemosensor but also the UV and fluorescence properties of the neighboring anthracene ring.[18] In addition to

the chiroptical sensing of the ee, this would then enable one to determine the total concentration of the substrate directly from the optical response of **1**. Unfortunately, only a small increase in the UV and fluorescence signals of **1** was observed upon imine formation, and the changes were insufficient for quantitative analysis (see the Supporting Information).

Although the enantioselective sensing of various chiral compounds with **1** was quite encouraging, we concluded that the incorporation of a fluorophore that (a) provides less steric hindrance to the substrate fixation and (b) has a strong interaction with a bound substrate that results in a distinct and

Scheme 3. Synthesis of Sensor 2 and Crystal Structure of Intermediate 6[a]
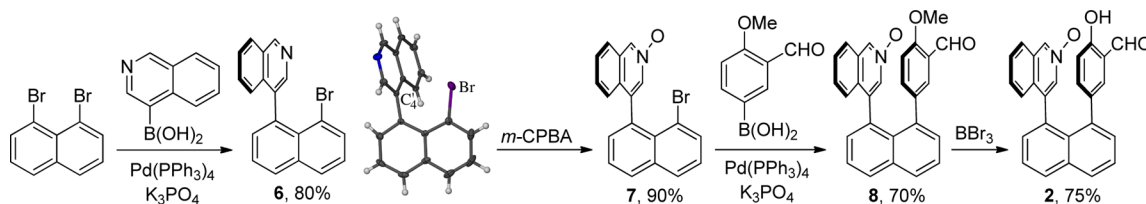
[a]Selected crystallographic measurements for **6**: through-space C'_4–Br separation, 3.073 Å; twisting angle, 9.5°; splaying angle, 8.6°.
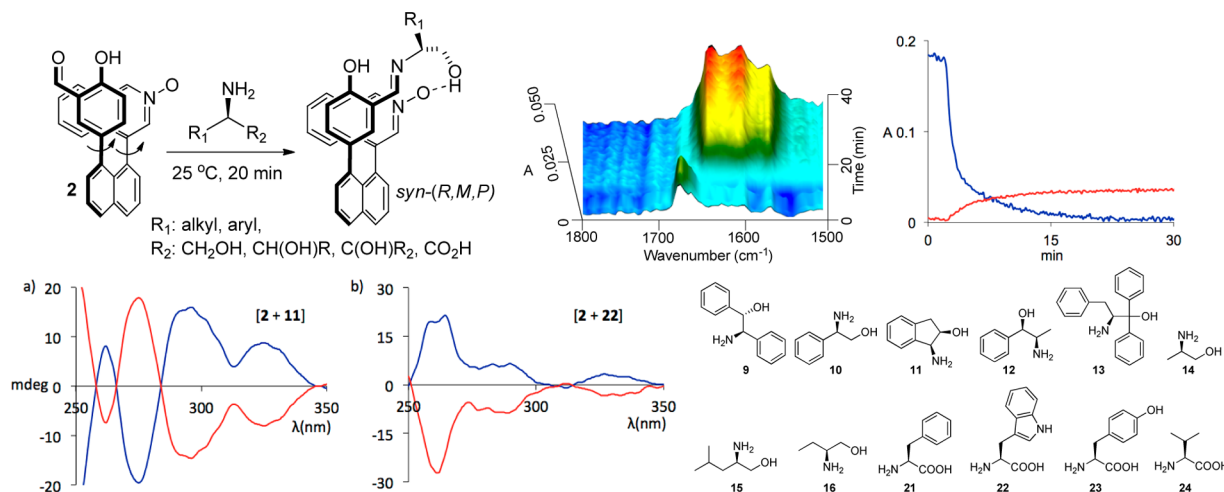

Figure 4. Top: Amino alcohol detection with sensor **2**. In-situ IR analysis of the condensation reaction between **2** and **10** and changes in the absorbance of the aldehyde stretching at 1680 cm^{-1} (red) and the imine stretching at 1640 cm^{-1} (blue) are shown. Bottom left: (a) CD spectra of the imines obtained from **2** and (1R,2R)-**11** (blue) and (1S,2S)-**11** (red). (b) CD spectra of the imines obtained from **2** and (R)-**22** (blue) and (S)-**22** (red). Bottom right: Substrate scope of sensor **2**. Only one enantiomer is shown.

quantifiable fluorescence response would afford a more useful chemosensor. We assumed that a fluorophore smaller than anthracene would not interfere with the imine formation step, thus significantly reducing the reaction time. The incorporation of a hydrogen-bond acceptor site in the fluorophore was expected to affect both the asymmetric induction process and the fluorescence response to the substrate binding event. These considerations led to the structure of sensor **2** carrying a salicylaldehyde ring for ee analysis and an isoquinoline N-oxide, a moderately sized fluorophore and hydrogen-bond acceptor, for total concentration analysis.

Determination of the Absolute Configuration, Enantiomeric Excess, and Total Amount of Chiral Compounds with Sensor 2. The experience obtained from the construction of the sterically crowded scaffold of **1** greatly facilitated the synthesis of **2**. In this case, however, we realized that the fluorophore had to be introduced first, followed by the attachment of the O-methylated salicylaldehyde unit (Scheme 3). The Suzuki cross-coupling of 1,8-dibromonaphthalene and 4-isoquinolineboronic acid largely left the second carbon–bromide bond intact and gave **6** in 80% yield. Oxidation with m-CPBA in dichloromethane afforded **7**, and the second Suzuki coupling with 3-formyl-4-methoxyphenylboronic acid provided **8** in 70% yield. The yields of both coupling steps were significantly higher than the aryl–aryl bond formations leading to compound **1**, which can be attributed to the reduced steric hindrance. The crystal structure of **6** also indicates a significantly smaller twisting angle between the bromine and the isoquinolyl ring. The demethylation with BBr$_3$ proceeded smoothly to give **2** under relatively mild conditions.

In-situ IR analysis of the condensation reaction between **2** and amino alcohol **10** showed that the imine formation proceeds rapidly, as indicated by the disappearance of the formyl stretching at 1680 cm^{-1} and the increase in the imine stretching at 1640 cm^{-1} (Figure 4). NMR and MS analysis confirmed complete conversion of the starting material within 20 min even in the absence of an acid catalyst. It is noteworthy that the rate of the condensation reaction between **10** and **2** was found to be greater than that with free salicylaldehyde under similar conditions, which required 2 h for complete conversion to the imine (see the Supporting Information). On the basis of the faster substrate binding with the isoquinoline N-oxide-derived probe **2**, we concluded that it would be a much more practical chemosensor than the sterically hindered prototype **1**, warranting a closer investigation of its (chir)optical sensing potential.

The CD spectra of the imines obtained from **2** and a wide variety of unprotected amino alcohols **9**−**16** and amino acids **21**−**24** were collected (Figure 4). The condensation reactions were carried out in chloroform, and the CD analyses were performed with diluted samples in hexanes. In contrast to the results obtained with sensor **1**, the CD amplitudes were diminished in alcoholic solvents such as methanol and ethanol. This is in perfect agreement with the anticipated intramolecular hydrogen-bonding motif between the alcohol or carboxylic acid moiety of the substrate and the N-oxide of the isoquinolyl unit in the chemosensor. The absolute configuration of the substrates can be consistently correlated with the sign of the CD signal at 260 nm, with R enantiomers generating a positive CD maximum and S enantiomers a negative one (entries 13−24 in Table 1).
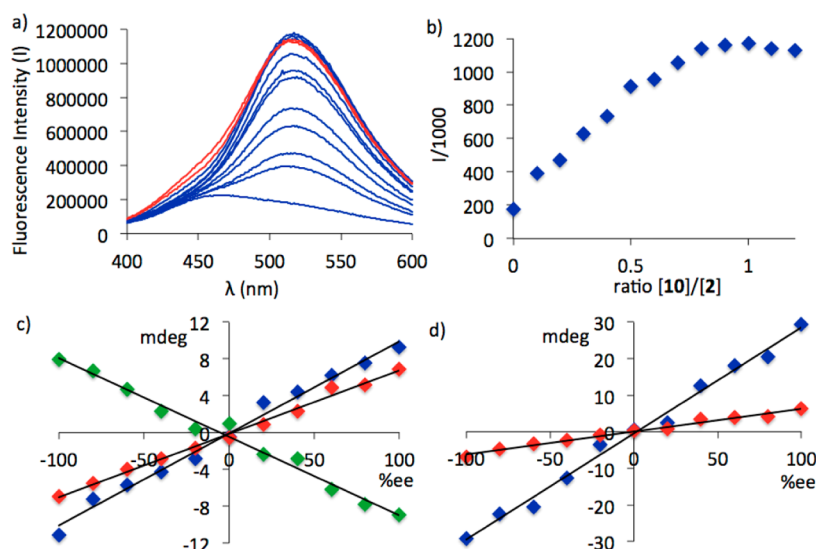
Figure 5. (a) Fluorescence spectra of **2** obtained upon addition of up to 1 equiv of **10** (blue) and in the presence of an excess of the amino alcohol (red). (b) Plot of the fluorescence intensity at 515 nm vs the [**10**]/[**2**] ratio. (c) Plots of the CD maxima of the phenylglycinol-derived imine of **2** at 275 nm (blue), 295 nm (red), and 325 nm (green) vs the % ee of substrate **10**. (d) Plots of the CD maxima of the tryptophan-derived imine at 275 nm (blue) and 295 nm (red) vs the % ee of **22**.

Table 2. Quantitative Enantiomeric Excess and Concentration Sensing of Substrates 10 and 22[a]

								chemosensing results						
				phenylglycinol (**10**)								tryptophan (**22**)		
	sample composition				ee (%)							ee (%)		
entry	conc (mM)	Ee (%)	abs config	conc (mM)	275 nm	295 nm	325 nm	avg	abs config	entry	260 nm	290 nm	avg	abs config
1	0.63	87.0	R	0.63	92.0	96.6	87.1	**91.9**	**R**	5	84.1	86.4	**85.3**	**R**
2	1.34	76.0	R	1.30	62.8	77.1	77.7	**72.5**	**R**	6	71.4	73.5	**72.5**	**R**
3	2.67	68.0	S	2.62	65.4	66.3	59.5	**63.7**	**S**	7	67.8	67.7	**67.8**	**S**
4	3.23	89.0	S	3.38	85.6	82.0	92.7	**86.8**	**S**	8	90.4	89.4	**89.9**	**S**

[a]See the Supporting Information for details.

Scheme 4. Asymmetric Transformation of the First Kind of the Salicylidenimine Obtained from Amino Alcohols and Sensor 2[a]
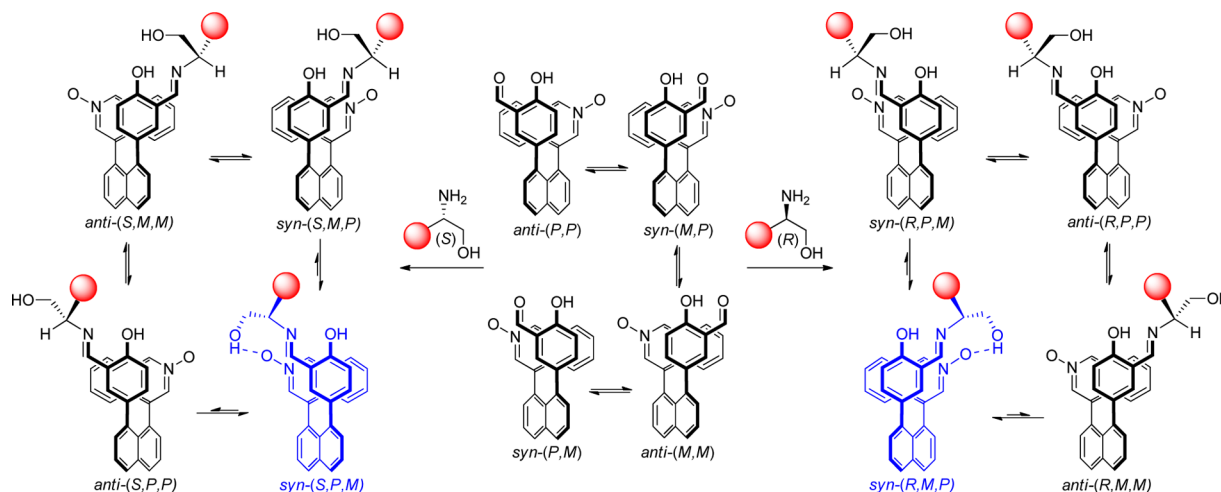
[a]The conformation that is stabilized by intramolecular hydrogen bonding and has the least steric repulsion is shown in blue.

In order to test the usefulness of **2** for ee determination of amino alcohols, CD spectra of the imines obtained with nonracemic samples of **10** covering a wide ee range were collected. Calibration curves were then constructed by plotting the intensity of the Cotton effects at three different wavelengths versus the substrate ee (Figure 5). On the basis of the linear regression equations derived from the calibration curves, the enantiomeric compositions of four unknown samples were determined (Table 2, entries 1−4). The average of the three values obtained from the CD readouts at 275, 295, and 325 nm gave the corresponding ee's with an accuracy that compares well with previously reported enantioselective chemosensing assays

and is sufficient for HTS purposes. Sensor **2** was also used successfully for ee determination of tryptophan (**22**). In this case, calibration curves were constructed for two different wavelengths, and the ee's of the unknown samples were calculated from the averages (Table 2, entries 5−8).

We were very pleased to find that **2** can also be used for the determination of the concentration of amino alcohols, which is another important advantage over chemosensor **1**. The fluorescence outputs of the imine obtained from **2** and **10** using varying amounts of **10** were measured. A steady fluorescence enhancement was observed upon addition of up to 1.0 molar equiv of the substrate, and the intensity remained nearly constant in the presence of excess **10** (Figure 5). The 6-fold increase in the fluorescence of **2** upon binding of **10** proved to be independent of the substrate chirality and allowed accurate determination of the concentration of the four nonracemic samples tested (Table 2). For example, the chemosensing of a 0.63 mM solution of **10** having 87.0% ee gave virtually the same concentration and 91.9% ee (entry 1 in Table 2). Similar results were obtained with the other samples, that is, the concentrations were generally determined with less than 5% error and the ee's were within a 6% margin. It is noteworthy that the accuracy of the ee and concentration analyses suffices for HTS purposes and compares well with results generally obtained with chemosensing assays.

A comparison of the chiroptical responses of chemosensors **1** and **2** reveals that the latter generates a lower CD readout upon detection of the amino alcohols **9** and **10** (compare entries 1 and 2 with entries 13 and 14 in Table 1). This may be attributed to the coexistence of several diastereomeric isomers, each having individual and possibly opposite CD effects. The free chemosensor **2** exists as a mixture of two diastereomeric pairs of enantiomers that undergo fast interconversion through rotation of both the salicylaldehyde and isoquinolyl *N*-oxide moieties about the chiral aryl−aryl bonds (Scheme 4). NMR analysis revealed the presence of diastereomeric *anti* and *syn* isomers in a 7:3 ratio, each being a racemic mixture in the absence of a chiral bias. Upon substrate binding, this equilibrium is disturbed, with the intramolecular hydrogen-bonding motif between the *N*-oxide and the alcohol of the substrate as well as steric effects favoring one conformer. For example, chirality imprinting with an (*R*)-amino alcohol is expected to favor population of the *syn*-(*R*,*M*,*P*) diastereomer, placing the steric bulk of the substrate away from the isoquinolyl *N*-oxide moiety and in the least sterically hindered direction, although other stereoisomers may also be present. Accordingly, condensation of **2** with an (*S*)-amino alcohol would favor the enantiomeric *syn*-(*S*,*P*,*M*) conformation.

The coexistence of diastereomeric conformations with individual chiroptical properties, however, ultimately limits the overall CD intensity. In fact, we found that the intramolecular hydrogen-bonding motif in the imine derived from **9** does not prevail in the solid state. Single crystals of the condensation product obtained from **2** and substrate (1*S*,2*R*)-**9** were grown by slow diffusion of hexanes into a concentrated chloroform solution (Figure 6). Crystallographic analysis revealed an *anti* orientation of the cofacial aryl rings, which places the steric bulk of the substrate opposite to the isoquinolyl moiety and results in a (1*S*,2*R*,*M*,*M*) configuration. The crystallization of this particular conformer may be a result of an asymmetric transformation of the second kind due to solid-state packing forces, and the (1*S*,2*R*,*M*,*P*) conformer exhibiting a hydrogen bond between the alcohol group of **9** and the *N*-oxide of **2** is still likely to coexist and possibly predominate in solution.
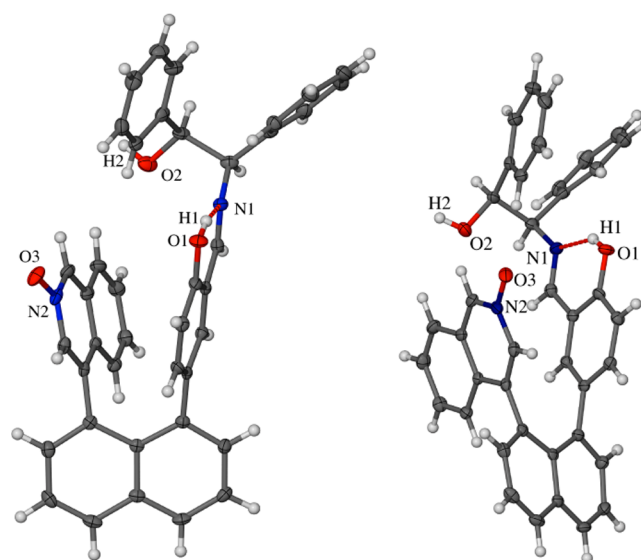

Figure 6. Front view (left) and side view (right) of the X-ray structure of the (1*S*,2*R*,*M*,*M*)-configured imine obtained from **2** and (1*S*,2*R*)-**9**. Selected crystallographic measurements: N1−H1, 1.773 Å; phenyl_centroid−isoquinolyl_centroid, 3.455 Å; twisting angle, 25.7°; splaying angle, 10.1°.

Development of Stereodynamic Sensor 3. The fast chirality sensing and accurate ee and concentration analysis of a variety of chiral compounds with probe **2** led to the design of 1-(3′-formyl-4′-methoxyphenyl)-8-(4′-pyridyl)naphthalene *N*-oxide (**3**). Sensor **3** combines the stereodynamic and (chir)-optical properties of **2** while exhibiting only one chiral axis, which reduces the number of possible diastereomeric conformations of the corresponding imine derivatives. We therefore anticipated that **3** would be as useful as **2** in enantioselective chemosensing applications and at the same time be more readily available and simplify the analysis of the chiral induction process. The synthesis of **3** in four steps and its use for sensing of amino alcohols were recently reported by our laboratory (Scheme 5).[9i] Chiroptical and crystallographic analysis of the condensation products obtained from **3** and amino alcohols provided evidence for a distinct asymmetric transformation of the first kind that is consistent with the chiral amplification model described above for sensor **2**. We found that the imine formation locks the stereodynamic scaffold of **3** into a single conformer that is stabilized by intramolecular hydrogen bonding between the substrate alcohol group and the pyridyl *N*-oxide moiety while the steric bulk of the bound imino alcohol moiety is placed into the least crowded direction (Scheme 5). This imprinting of the substrate chirality on the sensor structure occurs with excellent stereodivergence. Chiral amplification with an (*R*)-amino alcohol produces the *M* conformation and a positive CD response at 260 nm, while the *S* antipode leads to the corresponding *S*,*P* enantiomer and a negative CD maximum at the same wavelength (entries 25−33 in Table 1).

We now report that the chirality sensing scope of **3** extends to unprotected aliphatic and aromatic amino acids and that we observed a characteristic CD response at high wavelength that can be exploited for comprehensive chirality sensing (Figure 7).[19] In analogy to the substrate recognition capabilities of **2**, the condensation reaction using **3** as the probe is significantly faster than that with the bulky anthryl derivative **1**. In-situ IR, NMR, and MS analysis revealed that the substrate binding with **3** is complete within 15 min even in the absence of an acid catalyst,
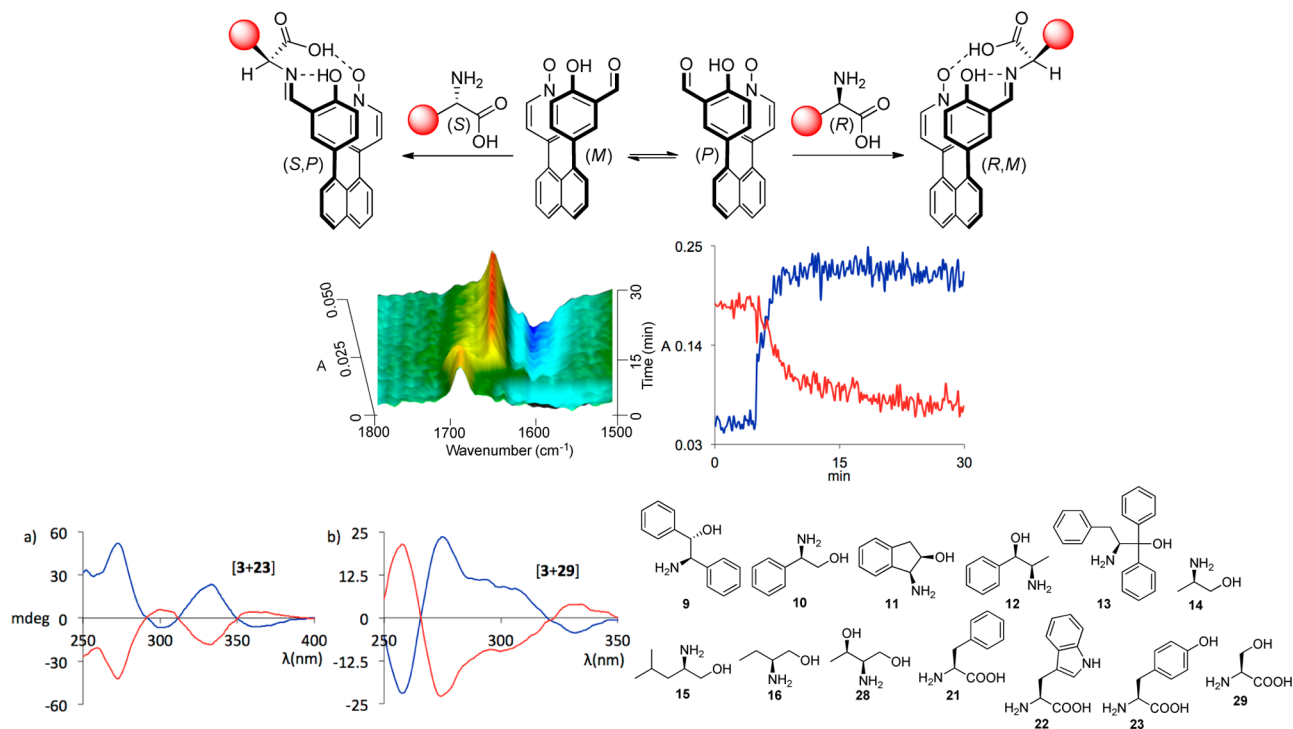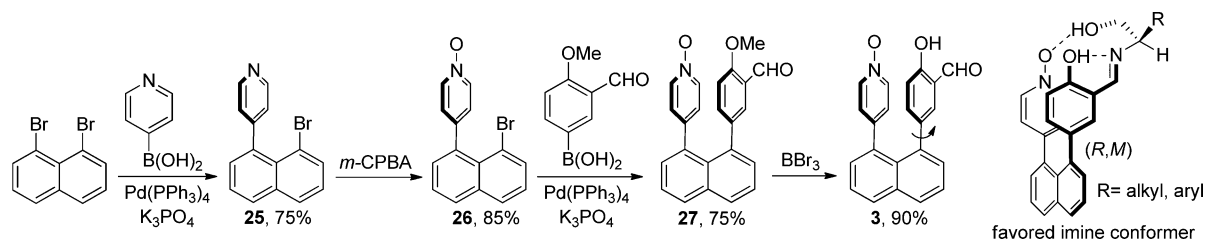
Scheme 5. Synthesis of 3 and Chiral Amplification with an (R)-Amino Alcohol[9i]

Figure 7. Top: Stereodivergence of the chirality imprinting of amino acids on sensor **3**. Middle: In-situ IR analysis of the condensation reaction between **3** and **10**. The disappearance of **3** was measured by the decrease in the absorbance intensity of the aldehyde stretching at 1685 cm^{-1} (red), and the generation of the imine was monitored by the increase in the absorbance intensity of the imine stretching at 1645 cm^{-1} (blue). Bottom left: (a) CD spectra of the imines obtained from **3** and (R)-**23** (blue) and (S)-**23** (red). (b) CD spectra of the imines obtained from **3** and (R)-**29** (blue) and (S)-**29** (red). All of the spectra were collected at 7.5×10^{-5} M in CHCl$_3$. Bottom right: Substrates tested with sensor **3**. Only one enantiomer is shown.

which proves its suitability for HTS purposes (see the Supporting Information). In accordance with the chiroptical sensing of amino alcohols, a positive CD response at 270 nm was consistently observed for R-configured amino acids, whereas the S antipodes yielded negative CD amplitudes at the same wavelength (entries 34−37 in Table 1). These results suggest that the binding of amino acids is followed by the same instantaneous chiral induction process. The binding of an (R)-amino acid by **3** thus leads to a predominant population of the R,M conformation, which is stabilized by intramolecular hydrogen bonding while steric repulsion between the amino acid residue and the sensor scaffold is kept at a minimum. The formation of the M conformer of the salicylidenimine derivative of **3** coincides with a positive CD response at 270 nm. Similarly, binding of an S-configured substrate favors the corresponding S,P enantiomer, which affords a negative CD maximum at the same wavelength (Figure 7).

We then applied **3** in the chirality, ee, and concentration analysis of tyrosine (**23**). Calibration curves constructed from the chiroptical response of **3** to nonracemic samples of **23** showed a linear relationship between the CD amplitudes at three different

wavelengths and the substrate ee (Figure 8). In addition, the fluorescence properties of the sensor changed significantly upon substrate binding. We observed that the intensity of the fluorescence signal of **3** at 450 nm steadily decreases in the presence of up to 1 molar equiv of tyrosine but remains constant when additional amounts of **23** are added. Interestingly, the fluorescence response of sensors **2** and **3** appears to depend on the class of compounds detected. As shown in Figure 5, the binding of phenylglycinol by **2** results in fluorescence enhancement, and a similar fluorescence change was obtained when sensor **3** was treated with an amino alcohol.[9i] By contrast, the binding of an amino acid causes fluorescence quenching. The imine derivatives of **2** and **3** formed with either phenylalanine or tyrosine show a remarkable decrease in the fluorescence intensity compared to the free sensor (Figures 8 and 19−21). Using the dual CD/fluorescence output of **3**, we were thus able to identify the absolute configuration of the major tyrosine enantiomer and to simultaneously determine the enantiomeric excess and the total amount of five samples covering wide concentration and ee ranges (Table 3).
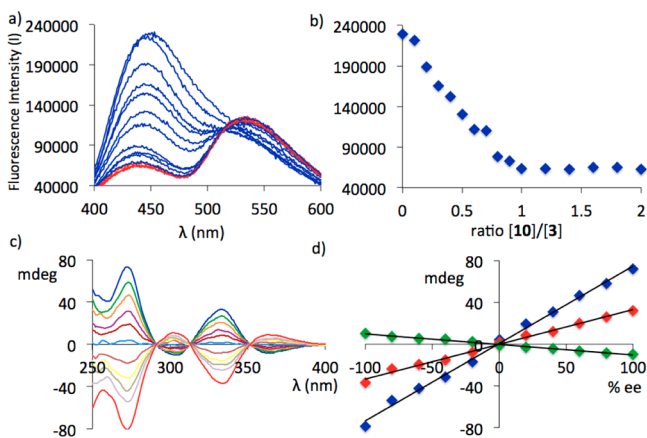
Figure 8. (a) Fluorescence spectra of **3** obtained upon addition of up to 1 equiv of **23** (blue) and in the presence of excess of the amino acid (red). (b) Plot of the fluorescence intensity at 450 nm vs the [**23**]/[**3**] ratio. (c) CD spectra of the imine obtained with nonracemic samples of **23**. (d) Plots of the CD maxima at 274 nm (blue), 305 nm (green), and 335 nm (red) vs the % ee of tyrosine.

Figure 9. (a) CD spectra of the imines obtained from **1** and (*R*)-**24** (solid blue) and (*S*)-**24** (solid red) in the presence of TBAOH and the CD response upon addition of HCl (dashed lines). (b) CD spectra of the imines obtained from **2** and (*R*)-**22** (solid blue) and (*S*)-**22** (solid red) in the presence of TBAOH and the CD response upon addition of HCl (dashed lines). (c) CD spectra of the imines obtained from **3** and (*R*)-**29** (solid blue) and (*S*)-**29** (solid red) in the presence of TBAOH and the CD response upon addition of HCl (dashed lines).

The CD sensing of amino acids with the triaryl probes **2** and **3** proved to be pH-sensitive, which is in accordance with the general importance of intramolecular hydrogen bonding between the bound substrate and the heteroaryl *N*-oxide units (Figure 9 and the Experimental Section). While the CD response of the imine obtained from **1** and **24** did not change upon addition of 1 equiv of HCl, the intensities of the Cotton effects measured for amino acid-derived condensation products of **2** and **3** increased significantly. In the presence of base, the free carboxylate group of the bound amino acid cannot participate in intramolecular hydrogen bonding with the neighboring heteroaryl *N*-oxide group. However, the generation of the free carboxylic acid function upon acidification enables intramolecular hydrogen bonding with the *N*-oxide moiety of **2** and **3**. As a result, a more distinct asymmetric transformation of the first kind favors population of the conformer showing the hydrogen-bonding motif, which ultimately leads to a stronger CD effect (Figure 7).

■ CONCLUSION

The incorporation of a salicylaldehyde ring and a neighboring aryl or heteroaryl chromophore at the peri positions of naphthalene affords stereodynamic circular dichroism/fluorescence sensors that can be used for rapid determination of the absolute configuration, enantiomeric excess, and total concentration of a variety of amines, amino alcohols, and amino acids at micromolar concentrations. The imine formation at the salicylaldeh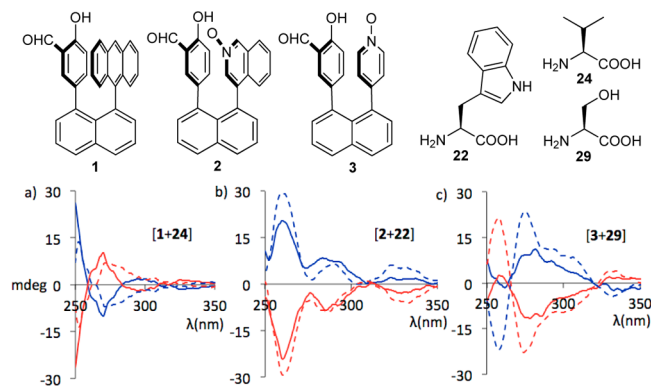yde unit initiates a spontaneous chiral amplification process that favors population of an axially chiral sensor conformation. This asymmetric transformation of the first kind turns on a characteristic chiroptical response from the sensor moiety that is correlated to the chirality and ee of the bound substrate. The covalent fixation of the substrate at the salicylaldehyde moiety is also recognized by the adjacent chromophore, thus inducing a strong change in the fluorescence output of the sensor. Because this second response is not stereoselective, it can be used to quantify the total amount of the substrate present in solution. This dual response sensor design has several attractive features: The substrate binding is fast and can be accelerated with catalytic amounts of acid if needed; the (chir)optical readouts occur at high wavelengths, which avoids interference with (chiral) impurities; micromolar sensor and substrate concentrations suffice for accurate determination of ee and concentration; the sensing method is operationally simple and suitable to automation and high-throughput screening applications; time-consuming product purification is not necessary, which allows convenient in situ analysis; and solvent waste production is reduced compared with chromatographic methods.

■ EXPERIMENTAL SECTION

1. General Information. All of the reagents and solvents were commercially available and used without further purification. Reactions were carried out under an inert atmosphere and anhydrous conditions. Flash chromatography was performed on silica gel (particle size 40−63 μm). NMR spectra were obtained at 400 MHz (^{1}H NMR) and 100 MHz

Table 3. Quantitative Enantiomeric Excess and Concentration Sensing of Tyrosine (23)[a]

| | sample composition | | | chemosensing results | | | | | |
| | | | | | ee (%) | | | | |
entry	conc (mM)	ee (%)	abs config	conc (mM)	274 nm	303 nm	335 nm	avg	abs config
1	0.56	87.0	*R*	**0.59**	87.4	88.3	90.1	**88.6**	*R*
2	1.01	76.0	*R*	**1.08**	74.2	73.8	76.7	**74.9**	*R*
3	1.73	12.0	*R*	**1.73**	11.8	13.2	12.9	**12.6**	*R*
4	2.36	26.0	*S*	**2.32**	27.1	28.3	25.3	**26.9**	*S*
5	2.93	68.0	*S*	**2.97**	66.3	65.4	66.8	**66.2**	*S*

[a]See the Supporting Information for details.

(¹³C NMR) using CDCl₃ as the solvent and TMS as the reference. Sensor **3** was prepared as previously reported.[9i] The quantum yields of **1**−**3** were determined in chloroform as 0.2%, 0.4%, and 0.05%, respectively, following literature procedures.[20]

2. Syntheses of 1-(3′-Formyl-4′-hydroxyphenyl)-8-(9′-anthryl)naphthalene (1) and 1-(4′-Isoquinolyl)-8-(3′-formyl-4′-hydroxyphenyl)naphthalene *N*-Oxide (2). *1-(3′-Formyl-4′-methoxyphenyl)-8-bromonaphthalene (4).* A solution of 1,8-dibromonaphthalene (500 mg, 1.7 mmol), 3-formyl-4-methoxyphenylboronic acid (472.0 mg, 2.6 mmol), Pd(PPh₃)₄ (151.5 mg, 0.13 mmol), and K₃PO₄ (927.7 mg, 4.4 mmol) in 18 mL of toluene/ethanol/water (3:2:1 v/v) was stirred at 80 °C for 4 h. The resulting mixture was allowed to cool to room temperature, quenched with water, and extracted with CH₂Cl₂. The combined organic layers were dried over MgSO₄ and concentrated in vacuo. Purification by flash chromatography on silica gel (CH₂Cl₂/hexanes 4:1) afforded 417 mg (1.2 mmol, 70% yield) of a yellow solid.

¹H NMR: δ 4.02 (s, 3H), 7.12 (d, *J* = 8.5 Hz, 1H), 7.39−7.50 (m, 3H), 7.68 (d, *J* = 8.2 Hz, 1H), 7.81 (dd, *J* = 8.4 Hz, 8.2 Hz, 2H), 7.90 (d, *J* = 8.0 Hz, 1H), 7.98 (s, 1H), 10.56 (s, 1H). ¹³C NMR: δ 55.8, 110.7, 119.8, 124.0, 125.3, 126.1, 129.0, 129.1, 129.5, 129.8, 131.4, 133.8, 135.3, 136.1, 137.4, 138.6, 161.1, 190.0. Mp: 194−195 °C. Anal. Calcd for C₁₈H₁₃BrO₂: C, 63.36; H 3.84. Found: C, 63.18; H, 4.06.

1-(3′-Formyl-4′-methoxyphenyl)-8-(9′-anthryl)naphthalene (5). A solution of **3** (400 mg, 1.2 mmol), anthracene-9-boronic acid (390 mg, 1.8 mmol), Pd(PPh₃)₄ (208 mg, 0.2 mmol), and K₃PO₄ (636.8 mg, 3.0 mmol) in 15 mL of toluene was stirred at 120 °C for 18 h. The resulting mixture was allowed to cool to room temperature, quenched with water, and extracted with CH₂Cl₂. The combined organic layers were dried over MgSO₄ and concentrated in vacuo. Purification by flash chromatography on silica gel (CH₂Cl₂/hexanes 4:1) afforded 206 mg (0.5 mmol, 40% yield) of a yellow solid.

¹H NMR: δ 3.61 (s, 3H), 5.53 (d, *J* = 8.5 Hz, 1H), 6.30 (dd, *J* = 8.5 Hz, 2.2 Hz, 1H), 6.63 (d, *J* = 2.1 Hz, 1H), 7.08 (d, *J* = 7.0 Hz, 1H), 7.20−7.41 (m, 7H), 7.49 (dd, *J* = 7.7 Hz, 7.5 Hz, 1H), 7.63 (dd, *J* = 7.8 Hz, 7.4 Hz, 1H), 7.78 (d, *J* = 8.5 Hz, 1H), 7.84 (d, *J* = 8.5 Hz, 1H), 8.05−8.08 (m, 2H), 8.11 (d, *J* = 8.2 Hz, 1H), 9.63 (s, 1H). ¹³C NMR: δ 55.3, 108.0, 121.4, 124.7, 125.0, 125.1, 125.3, 125.4, 125.7, 125.9, 126.9, 127.1, 127.7, 127.8, 127.9, 129.2, 129.4, 130.0, 130.7, 130.9, 131.2, 131.3, 131.8, 132.0, 133.8, 134.7, 135.0, 135.6, 137.5, 139.1, 158.8, 188.4. Mp: 188−189 °C. Anal. Calcd for C₃₂H₂₂O₂: C, 87.65; H, 5.06. Found: C, 87.85; H, 5.27.

1-(3′-Formyl-4′-hydroxyphenyl)-8-(9′-anthryl)naphthalene (1). A solution of **4** (200 mg, 0.46 mmol) and LiCl (193 mg, 4.6 mmol) in 5 mL of DMF was stirred at 150 °C for 12 h. The resulting mixture was allowed to cool to room temperature, quenched with water, and extracted with CH₂Cl₂. The combined organic layers were washed with brine, dried over MgSO₄, and concentrated in vacuo. Purification by flash chromatography on silica gel (CH₂Cl₂/hexane 2:1) afforded 87.1 mg (0.2 mmol, 60% yield) of a yellow solid.

¹H NMR: δ 5.65 (d, *J* = 8.4 Hz, 1H), 6.26 (d, *J* = 2.2 Hz, 1H), 6.30 (dd, *J* = 8.4 Hz, 2.3 Hz, 1H), 7.07 (d, *J* = 7.0 Hz, 1H), 7.19−7.38 (m, 5H), 7.44 (d, *J* = 8.3 Hz, 1H), 7.48−7.53 (m, 2H), 7.66 (dd, *J* = 8.1 Hz, 8.0 Hz, 1H), 7.81 (ddd, *J* = 8.6 Hz, 8.5 Hz, 2.9 Hz, 2H), 8.06 (d, *J* = 8.3 Hz, 1H), 8.11−8.14 (m, 2H), 8.56 (s, 1H), 10.42 (s, 1H). ¹³C NMR: δ 113.7, 117.2, 124.8, 124.9, 125.0, 125.2, 125.4, 125.5, 126.0, 126.7, 127.1, 128.4, 128.5, 129.4, 129.5, 130.2, 130.8, 130.9, 131.2, 131.3, 131.8, 132.1, 132,3, 132.9, 135.0, 135.1, 135.5, 137.4, 138.8, 158.9, 195.6. Mp: 199−200 °C. Anal. Calcd for C₃₁H₂₀O₂: C, 87.71; H, 4.75. Found: C, 87.97; H, 5.08.

1-Isoquinolyl-8-bromonaphthalene (6). A solution of 1,8-dibromonaphthalene (500 mg, 1.7 mmol), 4-isoquinolineboronic acid (453.7 mg, 2.6 mmol), Pd(PPh₃)₄ (151.5 mg, 0.13 mmol), and K₃PO₄ (927.7 mg, 4.4 mmol) in 18 mL of toluene/ethanol/water (3:2:1 v/v) was stirred at 80 °C for 4 h. The resulting mixture was allowed to cool to room temperature, quenched with water, and extracted with CH₂Cl₂. The combined organic layers were dried over MgSO₄ and concentrated in vacuo. Purification by flash chromatography on silica gel (CH₂Cl₂/EtOAc 2:1) afforded 470 mg (1.4 mmol, 80% yield) of a yellow solid.

¹H NMR: δ 7.26−7.36 (m, 2H), 7.51−7.61 (m, 4H), 7.71 (d, *J* = 7.4 Hz, 1H), 7.95 (d, *J* = 8.0 Hz, 1H), 8.01 (dd, *J* = 9.3 Hz, 9.3 Hz, 2H), 8.48

(s, 1H), 9.33 (s, 1H). ¹³C NMR: δ 119.7, 125.2, 125.5, 126.4, 127.0, 127.5, 127.8, 129.2, 130.1, 130.3, 130.6, 132.1, 133.9, 134.0, 134.2, 136.0, 136.6, 143.2, 151.7. Mp: 170−171 °C. Anal. Calcd for C₁₉H₁₂BrN: C, 68.28; H, 3.62; N, 4.19. Found: C, 68.07; H, 3.62; N, 4.13.

*1-(4′-Isoquinolyl)-8-bromonaphthalene *N*-Oxide (7).* A solution of **5** (470 mg, 1.4 mmol) and *m*-CBPA (728 mg, 4.2 mmol) in 15 mL of CH₂Cl₂ was stirred at room temperature for 12 h. The mixture was washed with 2 M NaOH, dried over MgSO₄, and concentrated in vacuo. Purification by flash chromatography on silica gel (CH₂Cl₂/MeOH 20:1) afforded 441 mg (1.26 mmol, 90% yield) of a light-brown solid.

¹H NMR: δ 7.14 (d, *J* = 8.5 Hz, 1H), 7.34−7.42 (m, 2H), 7.48 (d, *J* = 7.1 Hz, 1H), 7.56−7.62 (m, 2H), 7.75 (d, *J* = 7.6 Hz, 1H), 7.77 (d, *J* = 8.4 Hz, 1H), 7.96 (d, *J* = 8.6 Hz, 1H), 8.05 (d, *J* = 8.9 Hz, 1H), 8.16 (s, 1H), 8.85 (s, 1H). ¹³C NMR: δ 119.2, 125.0, 125.5, 126.8, 128.9, 128.9, 129.2, 129.3, 130.1, 130.9, 131.1, 131.1, 131.9, 134.2, 135.3, 135.9, 136.9, 138.8. Mp: 99−100 °C. Anal. Calcd for C₁₉H₁₂BrNO: C, 65.16; H, 3.45; N, 4.00. Found: C, 65.14; H, 3.75; N, 3.84.

*1-(4′-Isoquinolyl)-8-(3′-formyl-4′-methoxyphenyl)naphthalene *N*-Oxide (8).* A solution of **6** (440 mg, 1.3 mmol), 3-formyl-4-methoxyphenylboronic acid (339.2 mg, 1.9 mmol), Pd(PPh₃)₄ (109 mg, 0.1 mmol), and K₃PO₄ (669 mg, 3.2 mmol) in 18 mL of toluene/ethanol/water (3:2:1 v/v) was stirred at 100 °C for 12 h. The resulting mixture was allowed to cool to room temperature, quenched with water, and extracted with CH₂Cl₂. The combined organic layers were dried over MgSO₄ and concentrated in vacuo. Purification by flash chromatography on silica gel (CH₂Cl₂/MeOH 20:1) afforded 357.6 mg (0.88 mmol, 70% yield) of a light-brown solid. NMR analysis showed a mixture of *syn* and *anti* isomers with a ratio of 80:20.

¹H NMR: δ 3.71 (s, 0.6H), 3.89 (s, 2.4H), 6.01 (d, *J* = 8.8 Hz, 0.2H), 6.64 (d, *J* = 7.7 Hz, 0.2H), 6.70 (d, *J* = 8.8 Hz, 0.8H), 6.90 (s, 0.8H), 6.99 (d, *J* = 8.0 Hz, 1H), 7.10 (d, *J* = 7.7 Hz, 0.8H), 7.27−7.31 (m, 2H), 7.39−7.48 (m, 3.2H), 7.56−7.65 (m, 2H), 7.94 (s, 1H), 8.02 (d, *J* = 7.7 Hz, 1H), 8.11 (d, *J* = 7.7 Hz, 1H), 8.37 (s, 1H), 9.92 (s, 0.8H), 10.36 (s, 0.2H). ¹³C NMR: δ 56.0, 109.2, 114.2, 122.2, 124.2, 125.3, 125.7, 125.8, 128.3, 128.8, 129.1, 129.2, 129.7, 130.2, 130.9, 130.9, 131.0, 133.5, 134.1, 134.7, 134.8, 136.5, 137.4, 138.1, 139.5, 159.9, 188.2. Mp: 194−195 °C. Anal. Calcd for C₂₇H₁₉NO₃: C, 79.98; H, 4.72; N, 3.45. Found: C, 79.85; H, 4.92; N, 3.45.

*1-(4′-Isoquinolyl)-8-(3′-formyl-4′-hydroxyphenyl)naphthalene *N*-Oxide (2).* A solution of **7** (350 mg, 0.86 mmol) and BBr₃ (1 M in CH₂Cl₂, 2.6 mL, 2.6 mmol) in 10 mL of CH₂Cl₂ was stirred at room temperature for 2 h. The resulting mixture was quenched with 2-propanol, washed with water, dried over MgSO₄, and concentrated in vacuo. Purification by flash chromatography on silica gel (CH₂Cl₂/MeOH 20:1) afforded 253 mg (0.65 mmol, 75% yield) of a white solid. NMR analysis showed a mixture of *syn* and *anti* isomers with a ratio of 70:30.

¹H NMR: δ 5.96 (d, *J* = 8.4 Hz, 0.3H), 6.59 (s, 1H), 6.69 (d, *J* = 8.4 Hz, 0.7H), 7.06−7.17 (m, 2H), 7.27−7.48 (m, 2H), 7.66−7.87 (m, 5H), 7.89−7.92 (m, 1H), 8.04 (d, *J* = 8.10 Hz, 1H), 8.12 (d, *J* = 8.1 Hz, 1H), 8.34 (s, 0.3H), 8.44 (s, 0.7H), 9.08 (s, 0.7H), 9.82 (s, 0.3H), 10.60 (s, 0.7H), 10.98 (s, 0.3H). ¹³C NMR: δ 114.7, 115.2, 117.9, 124.9, 125.3, 125.6, 125.7, 126.0, 128.3, 128.7, 128.9, 129.0, 129.3, 129.3, 129.4, 129.4, 130.7, 130.8, 130.9, 131.0, 131.0, 132.9, 133.0, 134.2, 134.7, 134.9, 136.4, 136.8, 137.0, 137.8, 137.8, 139.2, 139.2, 159.2, 159.8, 195.2, 196.0. Mp: 232−233 °C. Anal. Calcd for C₂₆H₁₇NO₃: C, 79.78; H, 4.38; N, 3.58. Found: C, 79.81; H, 4.72; N, 3.40.

3. Enantioselective CD Sensing Experiments. *3.1. General Procedure for Chemosensing of Amines and Amino Alcohols.* A stock solution of sensor **1** or **2** (0.00375 M) in CHCl₃ was prepared, and 350 μL portions were transferred to 4 mL vials. Solutions of the substrates (0.026 M in CHCl₃) were prepared. To each vial containing 350 μL of stock solution was added 1 equiv (50 μL, 0.0013 mmol) of the substrate. The reaction mixtures were stirred overnight for sensor **1** and 15 min for sensor **2**. The reaction times could be reduced to 5 h for sensor **1** by addition of 10 mol % trifluoroacetic acid or *p*-toluenesulfonic acid. The CD analysis was conducted with sample concentrations of 7.50 × 10⁻⁵ M in MeOH for sensor **1** and in hexanes for sensor **2**. CD spectra were collected with a standard sensitivity of 100 mdeg, a data pitch of 0.5 nm, a bandwidth of 1 nm, a scanning speed of 500 nm s⁻¹, and a response of

0.5 s using a quartz cuvette (1 cm path length). The data were baseline-corrected and smoothed using a binomial equation. Control experiments with free substrates showed no CD signal in the region of interest.

3.2. General Procedure for Chemosensing of Amino Acids. A stock solution of sensor **1**, **2**, or **3** (0.005 M) in DMSO was prepared, and 1 mL portions were transferred to 5 mL vials containing substrate **21**−**24** and **29** (0.005 mmol). Tetrabutylammonium hydroxide (1 M in methanol, 0.005 mmol, 5 μL) was then added. The reaction mixtures were stirred overnight for sensor **1** and 15 min for sensors **2** and **3**. CD analysis was conducted with sample concentrations of 7.50×10^{-5} M in CHCl$_3$ for all sensors, and the instrument settings were the same as described above.

3.3. Analysis of Solvent Effects. The imines obtained with sensor **1** and amino alcohols or amines showed solvent-dependent CD readouts. The imines derived from **9**, **10**, and **18** were formed as described above, and CD spectra were collected in CHCl$_3$ and methanol (Figures 10−12).
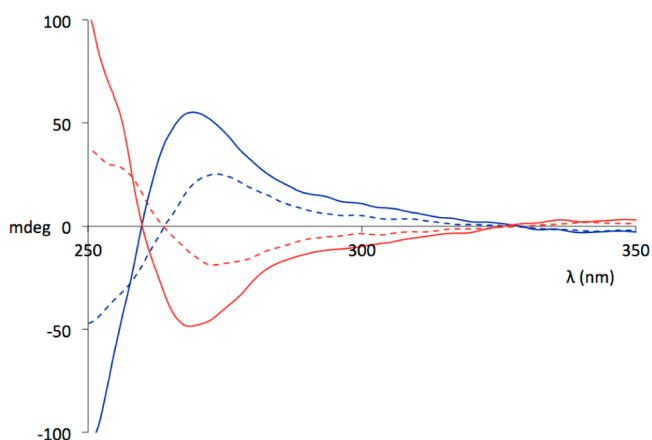
Figure 10. CD spectra of the imines obtained from **1** and (1*R*,2*R*)-**9** in CHCl$_3$ (dashed blue) or MeOH (solid blue) and (1*S*,2*S*)-**9** in CHCl$_3$ (dashed red) or MeOH (solid red).
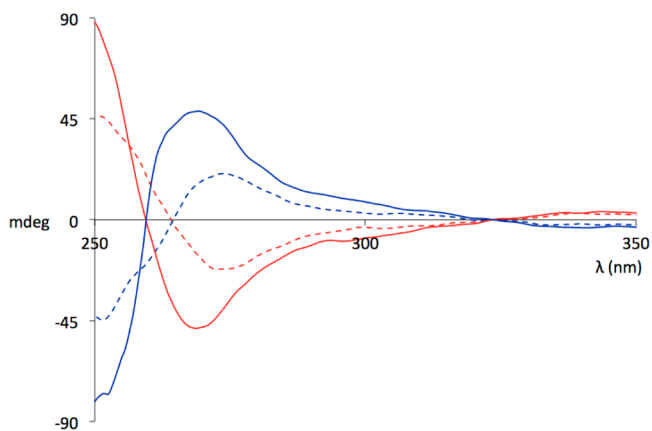

Figure 11. CD spectra of the imines obtained from **1** and (*R*)-**10** in CHCl$_3$ (dashed blue) or MeOH (solid blue) and (*S*)-**10** in CHCl$_3$ (dashed red) or MeOH (solid red).

3.4. Comparison of CD Outputs Obtained with the Protonated and Deprotonated Forms of the Imines Obtained from Sensors 1, 2, and 3 and Amino Acids. Imine formation with sensor **3** and amino acids **21**, **22**, **23**, and **29** was conducted in the presence of TBAOH as described above. After the condensation was complete, 1 equiv of HCl (1.25 M in EtOH, 4 μL) was added, changing the color from dark to light yellow. CD spectra were collected as described above (Figures 13−16).

The imine formation with sensor **2** and amino acid **22** was conducted in the presence of TBAOH as described above. After the condensation was complete, 1 equiv of HCl (1.25 M in EtOH, 4 μL) was added. and a CD spectrum was collected as described above (Figure 17).
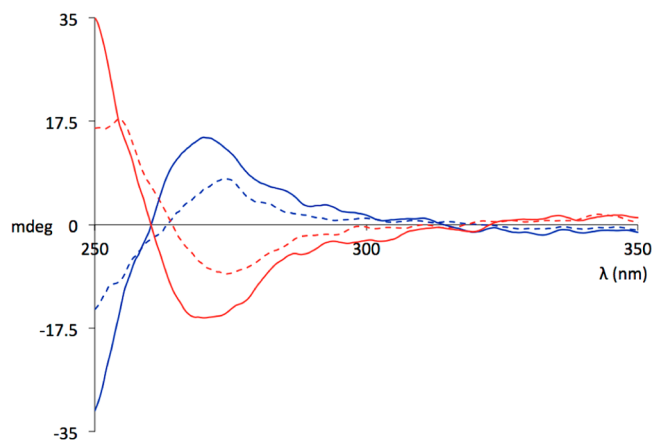

Figure 12. CD spectra of the imines obtained from **1** and (*R*)-**18** in CHCl$_3$ (dashed blue) or MeOH (solid blue) and (*S*)-**18** in CHCl$_3$ (dashed red) or MeOH (solid red).
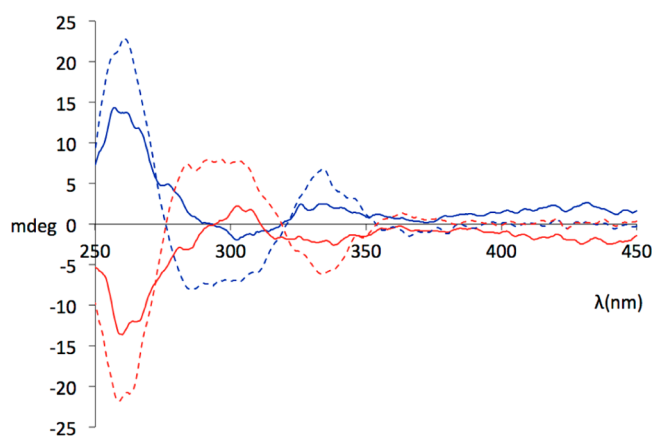

Figure 13. CD spectra of the imines obtained from **3**, TBAOH, and (*R*)-**21** (solid blue) and (*S*)-**21** (solid red) and CD responses of the imines obtained from **3** and (*R*)-**21** (dashed blue) and (*S*)-**21** (dashed red) upon addition of HCl.
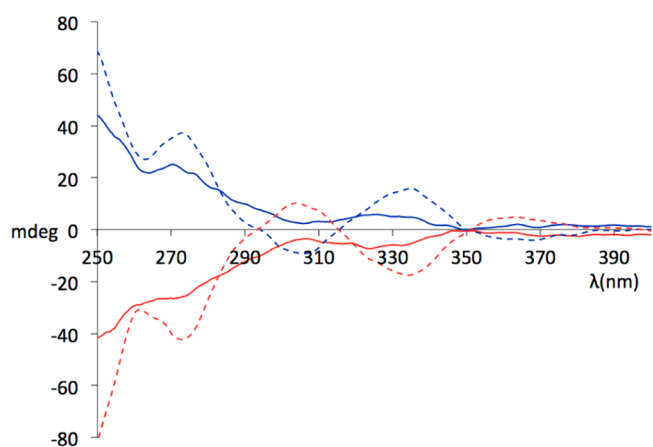

Figure 14. CD spectra of the imines obtained from **3**, TBAOH, and (*R*)-**22** (solid blue) and (*S*)-**22** (solid red) and CD responses of the imines obtained from **3** and (*R*)-**22** (dashed blue) and (*S*)-**22** (dashed red) upon addition of HCl.

The imine formation with sensor **1** and amino acid **24** was conducted in the presence of TBAOH as described above. After the condensation was complete, 1 equiv of HCl (1.25 M in EtOH, 4 μL) was added, and a CD spectrum was collected as described above (Figure 18).
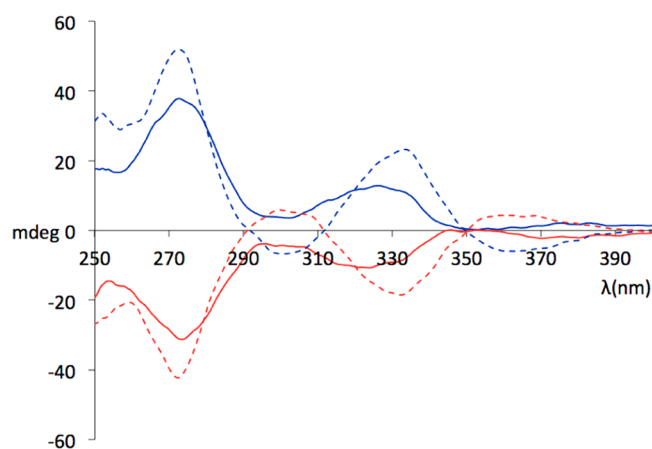
Figure 15. CD spectra of the imines obtained from **3**, TBAOH, and (*R*)-**23** (solid blue) and (*S*)-**23** (solid red) and CD responses of the imines obtained from **3** and (*R*)-**23** (dashed blue) and (*S*)-**23** (dashed red) upon addition of HCl.
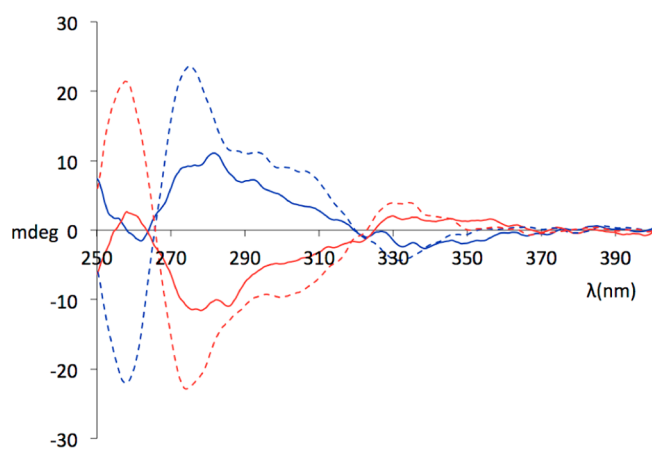

Figure 16. CD spectra of the imines obtained from **3**, TBAOH, and (*R*)-**29** (solid blue) and (*S*)-**29** (solid red) and CD responses of the imines obtained from **3** and (*R*)-**29** (dashed blue) and (*S*)-**29** (dashed red) upon addition of HCl.
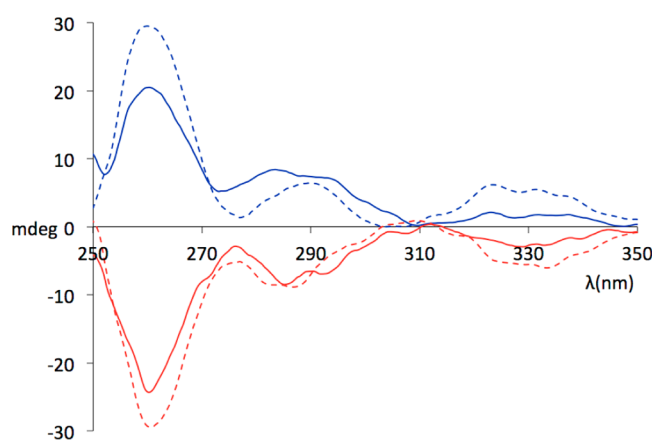

Figure 17. CD spectra of the imines obtained from **2**, TBAOH, and (*R*)-**22** (solid blue) and (*S*)-**22** (solid red) and CD responses of the imines obtained from **2** and (*R*)-**22** (dashed blue) and (*S*)-**22** (dashed red) upon addition of HCl.

4. Fluorescence Changes upon Imine Formation. To determine the impact of imine formation on the fluorescence of sensors **2** and **3**, fluorescence spectra were obtained for sensors **2** and **3** and the imines
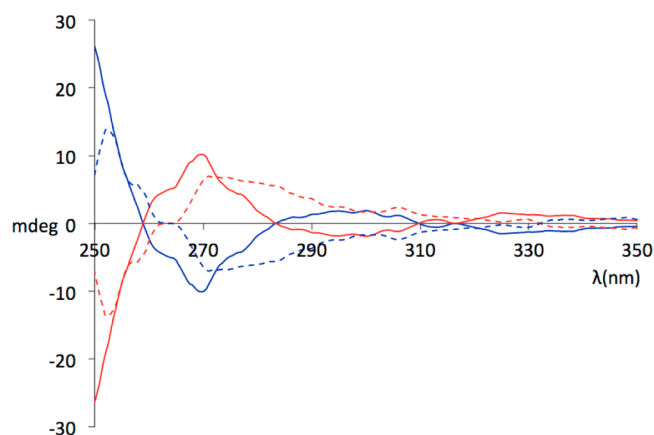

Figure 18. CD spectra of the imines obtained from **1**, TBAOH, and (*R*)-**24** (solid blue) and (*S*)-**24** (solid red) and CD responses of the imines obtained from **1** and (*R*)-**24** (dashed blue) and (*S*)-**24** (dashed red) upon addition of HCl.

obtained from **2** and phenylalanine, **2** and tyrosine, and **3** and phenylalanine. The results are shown in Figures 19−21.
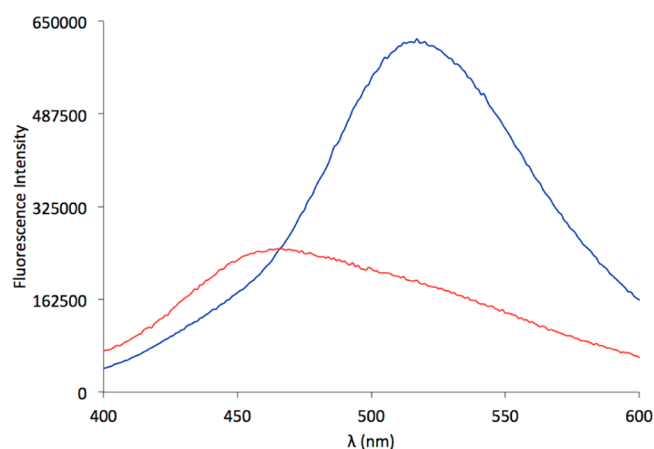

Figure 19. Fluorescence spectra obtained for sensor **2** (blue) and the imine obtained from **2** and 1 equiv of phenylalanine (red). Both spectra were collected in CHCl$_3$ (4.0×10^{-4} M) at an excitation wavelength of 340 nm.
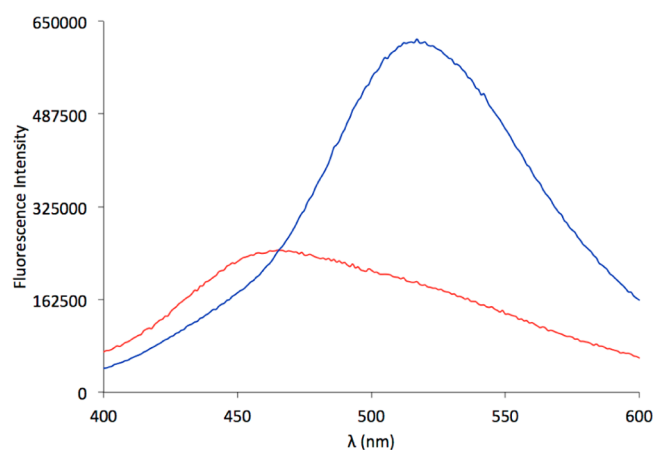

Figure 20. Fluorescence spectra obtained for sensor **2** (blue) and the imine obtained from **2** and 1 equiv of tyrosine (red). Spectra were collected in CHCl$_3$ (4.0×10^{-4} M) at an excitation wavelength of 340 nm.
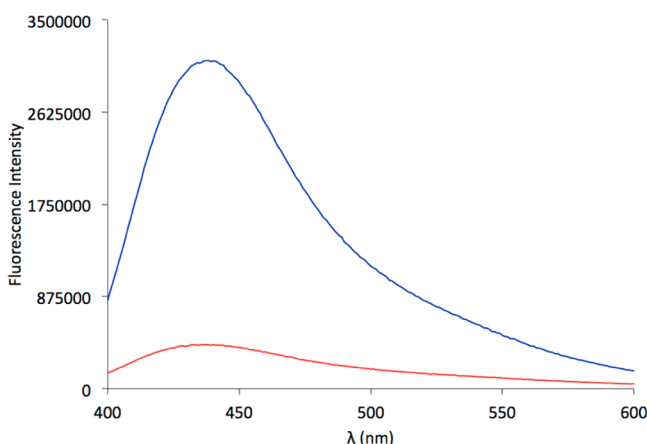
Figure 21. Fluorescence spectra obtained for sensor **3** (blue) and the imine obtained from **3** and 1 equiv of phenylalanine (red). Spectra were collected in $CHCl_3$ (4.0×10^{-4} M) at an excitation wavelength of 350 nm.

5. Determination of the Rotational Energy Barrier of Sensor 1 by Dynamic HPLC. The free energy barrier to rotation, $\Delta G^{\ddagger}$, of the 3′-formyl-4′-methoxyphenyl unit of sensor precursor **5** was determined by DHPLC. Compound **5** (1 mg, 0.002 mmol) was dissolved in 1.5 mL of CH_2Cl_2/hexanes (1:1 v/v). The HPLC analysis was performed using 1:1 CH_2Cl_2/hexanes as the mobile phase, a flow rate of 1 mL/min, an injection volume of 20 μL, and the (*S,S*)-Whelk-O 1 column as the chiral stationary phase at various temperatures. The rotational barrier was determined by simulation of the elution profiles obtained at −4.8, −10.4, −14.9, and −20.2 °C with the computer program Mimesis 3.1. The rate constant of enantiomerization was optimized until the simulated and experimentally obtained elution profiles were superimposable.

■ **ASSOCIATED CONTENT**

Ⓢ Supporting Information

Quantitative ee and concentration analysis; MS, CD, fluorescence, and NMR spectra; and crystallographic details (CIF). This material is available free of charge via the Internet at http://pubs.acs.org.

■ **AUTHOR INFORMATION**

Corresponding Author

*E-mail: cw27@georgetown.edu.

Notes

The authors declare no competing financial interest.

■ **ACKNOWLEDGMENTS**

■ **REFERENCES**

(1) Leung, D.; Kang, S. O.; Anslyn, E. V. *Chem. Soc. Rev.* **2012**, *41*, 448.

(2) (a) Matile, S.; Berova, N.; Nakanishi, K.; Novkova, S.; Philpova, I.; Blagoev, B. *J. Am. Chem. Soc.* **1995**, *117*, 7021. (b) Kurtan, T.; Nesnas, N.; Koehn, F. E.; Li, Y.-Q.; Nakanishi, K.; Berova, N. *J. Am. Chem. Soc.* **2001**, *123*, 5974. (c) Huang, X.; Fujioka, N.; Pescitelli, G.; Koehn, F. E.; Williamson, R. T.; Nakanishi, K.; Berova, N. *J. Am. Chem. Soc.* **2002**, *124*, 10320. (d) Balaz, M.; De Napoli, M.; Holmes, A. E.; Mammana, A.; Nakanishi, K.; Berova, N.; Purrello, R. *Angew. Chem., Int. Ed.* **2005**, *44*, 4006. (e) Berova, N.; Pescitelli, G.; Petrovic, A. G.; Proni, G. *Chem. Commun.* **2009**, 5958.

(3) (a) Superchi, S.; Casarini, D.; Laurita, A.; Bavoso, A.; Rosini, C. *Angew. Chem., Int. Ed.* **2001**, *40*, 451. (b) Superchi, S.; Bisaccia, R.; Casarini, D.; Laurita, A.; Rosini, C. *J. Am. Chem. Soc.* **2006**, *128*, 6893.

(c) Tartaglia, S.; Padula, D.; Scafato, P.; Chiummiento, L.; Rosini, C. *J. Org. Chem.* **2008**, *73*, 4865.

(4) (a) Nieto, S.; Lynch, V.; Anslyn, E.; Kim, H.; Chin, J. *J. Am. Chem. Soc.* **2008**, *130*, 9232. (b) Nieto, S.; Dragna, J.; Anslyn, E. *Chem.—Eur. J.* **2010**, *16*, 227. (c) Leung, D.; Anslyn, E. *Org. Lett.* **2011**, *13*, 2298. (d) Joyce, L. A.; Maynor, M. S.; Dragna, J. M.; da Cruz, G. M.; Lynch, V. M.; Canary, J. W.; Anslyn, E. V. *J. Am. Chem. Soc.* **2011**, *133*, 13746. (e) Joyce, L.; Canary, J.; Anslyn, E. *Chem.—Eur. J.* **2012**, *18*, 8064. (f) You, L.; Pescitelli, G.; Anslyn, E. V.; Di Bari, L. *J. Am. Chem. Soc.* **2012**, *134*, 7117. (g) You, L.; Berman, J. S.; Lucksanawichien, A.; Anslyn, E. V. *J. Am. Chem. Soc.* **2012**, *134*, 7126. (h) You, L.; Berman, J. S.; Anslyn, E. V. *Nat. Chem.* **2011**, *3*, 943.

(5) (a) Holmes, A.; Zahn, S.; Canary, J. *Chirality* **2002**, *14*, 471. (b) Holmes, A. E.; Das, D.; Canary, J. W. *J. Am. Chem. Soc.* **2007**, *129*, 1506. (c) Canary, J. W.; Mortezaei, S.; Liang, J. *Chem. Commun.* **2010**, *46*, 5850.

(6) (a) Yang, Q.; Olmsted, C.; Borhan, B. *Org. Lett.* **2002**, *4*, 3423. (b) Li, X.; Tanasova, M.; Vasileiou, C.; Borhan, B. *J. Am. Chem. Soc.* **2008**, *130*, 1885. (c) Li, X.; Borhan, B. *J. Am. Chem. Soc.* **2008**, *130*, 16126. (d) Li, X.; Burrell, C. E.; Staples, R. J.; Borhan, B. *J. Am. Chem. Soc.* **2012**, *134*, 9026. (e) Anyika, M.; Gholami, H.; Ashtekar, K. D.; Acho, R.; Borhan, B. *J. Am. Chem. Soc.* **2014**, *136*, 550.

(7) (a) Mazaleyrat, J.-P.; Wright, K.; Gaucher, A.; Toulemonde, N.; Wakselman, M.; Oancea, S.; Peggion, C.; Formaggio, F.; Setnicka, V.; Keiderling, T. A.; Toniolo, C. *J. Am. Chem. Soc.* **2004**, *126*, 12874. (b) Dutot, L.; Wright, K.; Gaucher, A.; Wakselman, M.; Mazaleyrat, J.-P.; De Zotti, M.; Peggion, C.; Formaggio, F.; Toniolo, C. *J. Am. Chem. Soc.* **2008**, *130*, 5986.

(8) (a) Sciebura, J.; Skowronek, P.; Gawronski, J. *Angew. Chem., Int. Ed.* **2009**, *48*, 7069. (b) Sciebura, J.; Gawronski, J. *Chem.—Eur. J.* **2011**, *17*, 13138.

(9) (a) Ghosn, M. W.; Wolf, C. *J. Am. Chem. Soc.* **2009**, *131*, 16360. (b) Ghosn, M. W.; Wolf, C. *J. Org. Chem.* **2011**, *76*, 3888. (c) Ghosn, M. W.; Wolf, C. *Tetrahedron* **2011**, *67*, 6799. (d) Iwaniuk, D. P.; Wolf, C. *J. Am. Chem. Soc.* **2011**, *133*, 2414. (e) Iwaniuk, D. P.; Wolf, C. *Org. Lett.* **2011**, *13*, 2602. (f) Iwaniuk, D. P.; Bentley, K. W.; Wolf, C. *Chirality* **2012**, *24*, 584. (g) Iwaniuk, D. P.; Wolf, C. *Chem. Commun.* **2012**, *48*, 11226. (h) Zhang, P.; Wolf, C. *Chem. Commun.* **2013**, *49*, 7010. (i) Bentley, K. W.; Wolf, C. *J. Am. Chem. Soc.* **2013**, *135*, 12200. (j) Bentley, K. W.; Wolf, C. *J. Am. Chem. Soc.* **2013**, *135*, 18052.

(10) (a) Kim, H.; So, S. M.; Yen, C. P.-H.; Vinhato, E.; Lough, A. J.; Hong, J.-I.; Kim, H.-J.; Chin, J. *Angew. Chem., Int. Ed.* **2008**, *47*, 8657. (b) Waki, M.; Abe, H.; Inouye, M. *Angew. Chem., Int. Ed.* **2007**, *46*, 3059. (c) Katoono, R.; Kawai, H.; Fujiwara, K.; Suzuki, T. *J. Am. Chem. Soc.* **2009**, *131*, 16896. (d) Wezenberg, S. J.; Salassa, G.; Escudero-Adan, E. C.; Benet-Buchholz, J.; Kleij, A. W. *Angew. Chem., Int. Ed.* **2011**, *50*, 713. (e) Kuwahara, S.; Nakamura, M.; Yamaguchi, A.; Ikeda, M.; Habata, Y. *Org. Lett.* **2013**, *15*, 5738. (f) Kim, M. J.; Choi, Y. R.; Jeon, H.-G.; Kang, P.; Choi, M.-G.; Jeong, K.-S. *Chem. Commun.* **2013**, *49*, 11412. For a review, see: (g) Wolf, C.; Bentley, K. W. *Chem. Soc. Rev.* **2013**, *42*, 5408. For chirality sensing based on CPL analysis, see: (h) Song, F.; Wei, G.; Jiang, X.; Li, F.; Cheng, Y.; Zhu, C. *Chem. Commun.* **2013**, *49*, 5772. For chirality sensing with helical microfibers, see: (i) Zou, W.; Yan, Y.; Fang, J.; Yang, Y.; Liang, J.; Deng, K.; Yao, J.; Wei, Z. *J. Am. Chem. Soc.* **2014**, *136*, 578.

(11) Attempts to reverse the coupling sequence and to install the anthracene unit prior to the salicylaldehyde moiety were unsuccessful because of prevailing debromination.

(12) Bao, K.; Fan, A.; Dai, Y.; Zhang, L.; Zhang, W.; Cheng, M.; Yao, X. *Org. Biomol. Chem.* **2009**, *7*, 5084.

(13) Yadav, J.; Reddy, B.; Madan, C.; Hashim, R. *Chem. Lett.* **2000**, *29*, 738.

(14) Du, Z. T.; Lu, J.; Yu, H. R.; Xu, Y.; Li, A. P. *J. Chem. Res.* **2010**, *34*, 222.

(15) Bernard, A.; Ghiani, R.; Piras, P.; Rivoldini, A. *Synthesis* **1989**, 287.

(16) In *Dynamic Stereochemistry of Chiral Compounds*; Wolf, C., Ed.; RSC Publishing: Cambridge, U.K., 2008; pp 84−94.

(17) The reaction time can be reduced to 90 min in the absence of an acid catalyst by microwave irradiation (chloroform at 100 °C, 100 W).

(18) (a) Cao, H.; Heagy, M. D. *J. Fluoresc.* **2004**, *14*, 569. (b) Martínez-Máñez, R.; Sancenón, F. *Chem. Rev.* **2003**, *103*, 4419. (c) Mei, X.; Wolf, C. *Chem. Commun.* **2004**, 2078. (d) Mei, X.; Wolf, C. *J. Am. Chem. Soc.* **2004**, *126*, 14736. (e) Mei, X.; Wolf, C. *J. Org. Chem.* **2005**, *70*, 2299.

(19) In contrast to sensor **1** carrying a bulky anthracene unit adjacent to the salicylaldehyde ring, the sterically less crowded probes **2** and **3** do not show a CD response upon binding of chiral amines. We believe that in the case of **2** and **3** the absence of the intramolecular hydrogen-bonding motif results in conformationally flexible imine derivatives that are CD-inactive because of insufficient central-to-axial chirality induction.

(20) Jones, G., II; Jackson, W. R.; Choi, C.-Y. *J. Phys. Chem.* **1985**, *89*, 294−300.